CHAPTER IV

RESULTS AND DISCUSSION

4.1 Effect of DEG stabilizing agent

4.1.1 Formation of crystal with DEG

4.1.1.1 Formation of crystal with different molar ratios of DEG

In this work, to investigate the effect of DEG on the formation of nanocrystal TiO_2, the different mole ratios of DEG were varied. However, the calcination temperature was kept constant at 450°C. The mole ratios of TTiP:DEG included 1:0, 1:0.5:, 1:1. 1:1.5, and 1:2.0. The crystal structures of TiO_2 from each condition obtaining from X-ray diffraction analysis are illustrated in Figure 4.1 and the corresponding surface morphology of TiO_2 nanocrystals are shown in Figure 4.2 (a)-(e).

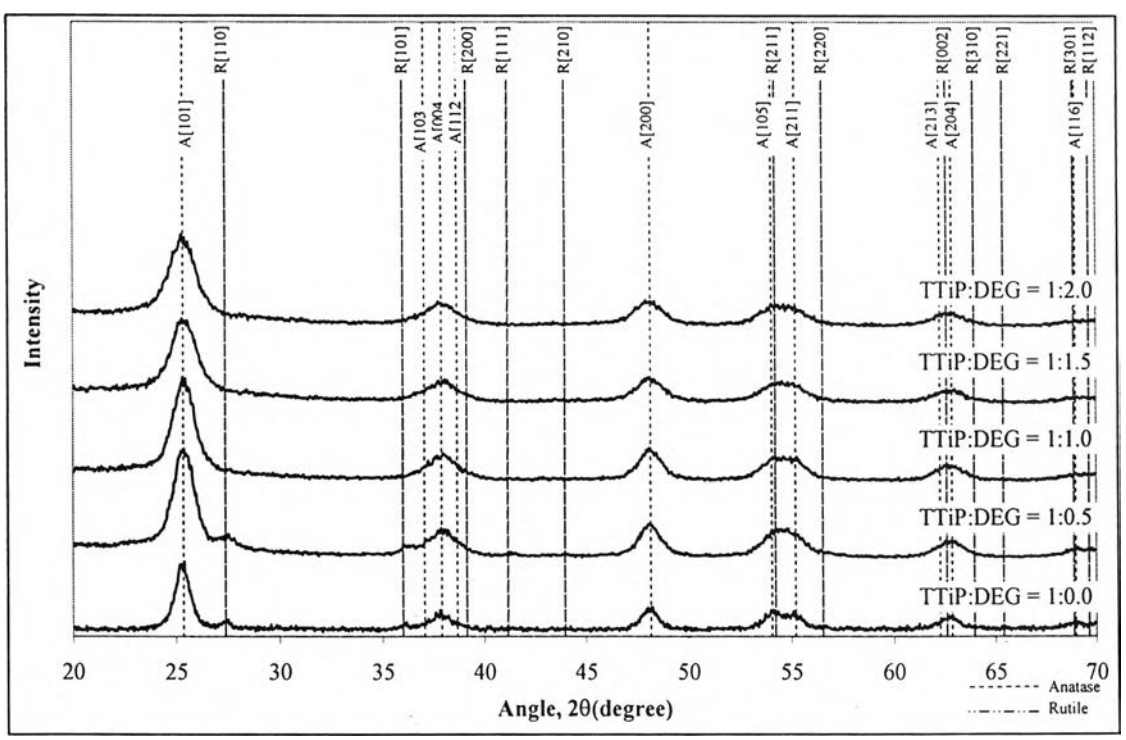

Figure 4.1 XRD spectrum showing crystal structures of TiO_2 obtained from different mole ratio of TTiP:DEG

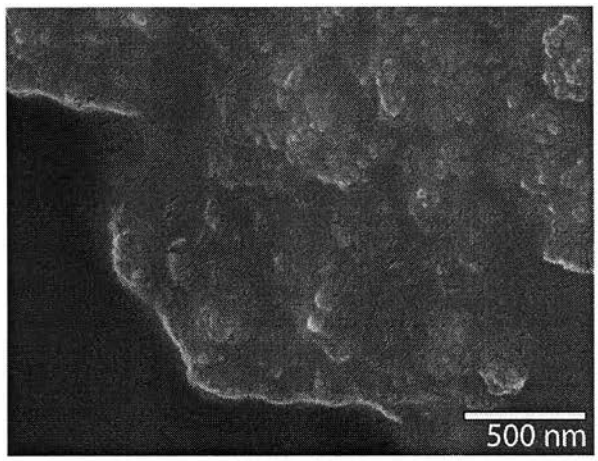

(a) TiO_2 without DEG

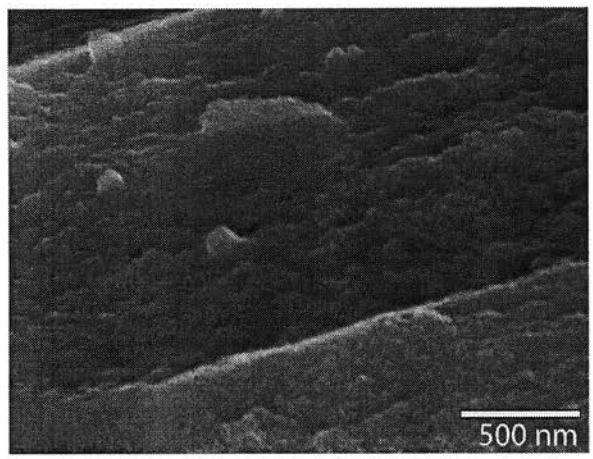

(b) TiO_2 with DEG, TTiP:DEG is 1:0.5

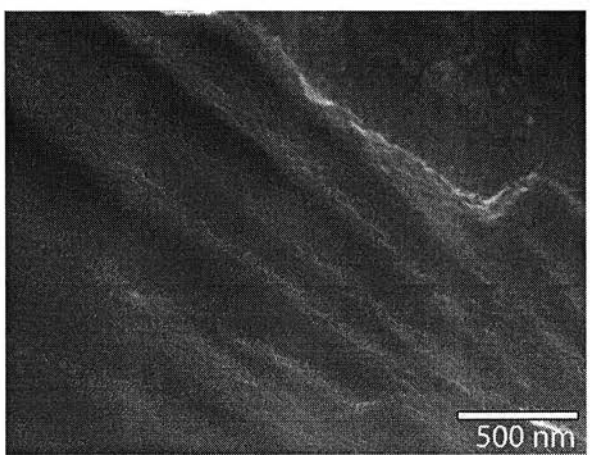

(c) TiO_2 with DEG, TTiP:DEG is 1:1.0

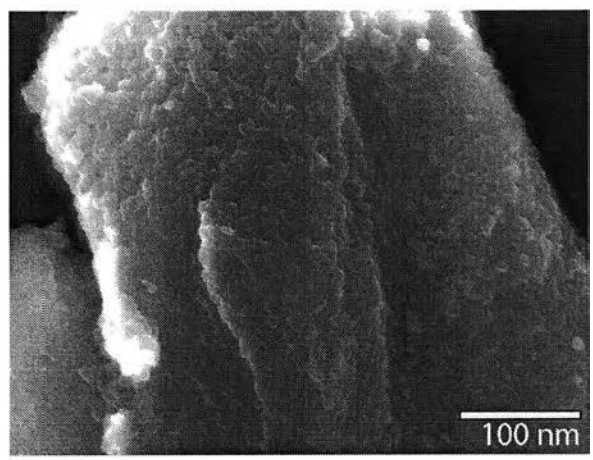

(d) TiO_2 with DEG, TTiP:DEG is 1:1.5

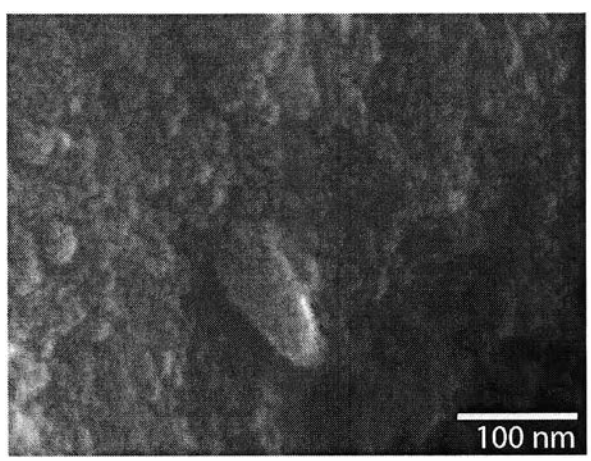

(e) TiO_2 with DEG, TTiP:DEG is 1:2.0

สำนักงานวิทยทรัพยากร
จุฬาลงกรณ์มหาวิทยาลัย

Figure 4.2 SEM images showing surface morphology of TiO_2 nanocrystals obtained from different mole ratios of TTiP:DEG

As shown in the X-ray diffraction patterns of TiO_2 nanoparticles in Figure 4.1, anatase phase was the predominant structure in all synthesis conditions. A major peak corresponding to (1 0 1) reflections of the anatase phase of TiO_2 is shown at the angle

of 25.36°, while the minor peaks are appeared at 48.15° and 54.05°. Peaks for rutile morphology could be found at the angle of 27.39°. It was also found that the intensity of anatase peaks is not significantly different as the molar ratio of DEG increased.

Moreover, DEG delays the phase transformation of anatase to rutile phase with mole ratio of TTiP:DEG higher than 1:0.5 as represented by X-ray diffraction pattern of TiO_2 nanoparticles in which a smaller amount of rutile was detected compared without DEG. To quantify the phase transformation from anatase to rutile with the different mole ratios of DEG, the percentage of anatase to rutile was calculated. The phase content of a sample can be calculated from the integrated intensities of the above-mentioned anatase, rutile, and brookite peaks. If a sample contains only anatase and rutile, the weight fraction of rutile (W_R) can be calculated from equation (Gribb and Banfield, 1997).

$$W_R = \frac{A_R}{0.884A_A + A_R} \tag{4.1}$$

where A_A represents the integrated intensity of the anatase (101) peak, and A_R the integrated intensity of rutile (110) peak. If brookite phase is also present in a sample, similar relations can be derived:

$$W_A = \frac{k_A A_A}{k_A A_A + A_R + k_B A_B} \tag{4.2}$$

$$W_R = \frac{A_R}{k_A A_A + A_R + k_B A_B} \tag{4.3}$$

$$W_B = \frac{k_B A_B}{k_A A_A + A_R + k_B A_B} \tag{4.4}$$

where W_A and W_B represent the weight fraction of anatase and brookite, respectively. A_B is the integrated intensity of the brookite (121) peak, and k_A and k_B are two coefficients to be determined where k_A = 0.886 and k_B = 2.721 (Zhang and Banfield, 2000).

Using above equations, the percentage values of anatase to rutile in each condition was calculated and shown in Table 4.1.

Table 4.1 Percentage of anatase and rutile phases in samples obtained with different mole ratios of TTiP:DEG

Mole ratio of TTiP:DEG	Anatase (%)	Rutile (%)
1:0	72.24	27.76
1:0.5	77.11	22.89
1:1.0	100.00	0.00
1:1.5	100.00	0.00
1:2.0	100.00	0.00

It was found that the percentage of anatase:rutile of TiO_2 without any stabilizing agents was calculated as equal to 72.24:27.76. With DEG addition in the ratio TTiP:DEG of 1:0.5, the percentage ratio of anatase:rutile was changed to be 77.11:22.89. Finally, the rutile phase not formed at all when TiO_2 was synthesized using 1:1.0 of the TTiP:DEG as 1:1.0. From this work, it is clear that one of the effects of DEG is delaying the phase transformation from anatase to rutile phase.

From microstructures of TiO_2 nanocrystals, shown in Figure 4.2, it is obvious that DEG also significantly reduce the size of the nanocrystals. As the amount of DEG increases, the size of the TiO_2 nanocrystal decreases. Compared to the morphology of TiO_2 without any stabilizing agents shown in Figure 4.2 (a), the size of TiO_2 with DEG is relatively smaller. To determine this sizing effect of DEG, crystallite sizes of TiO_2 were estimated from the broadening of corresponding X-ray diffraction peaks by Debye-Scherrer equation (Liqiang et al., 2003):

$$L = \frac{K\lambda}{\beta \cos\theta} \tag{4.5}$$

where L is the crystallite size, K usually taken as 0.89, λ is the wavelength of the X-ray radiation (0.15418 nm for $Cu_{K\alpha}$), β is the line width at half-maximum height and θ is the half diffraction angle of the centroid of the peak in degree. The crystal size of TiO_2 nanopowder as a function of mole ratio of TTiP:DEG is illustrated in Figure 4.3

In this work, it is found that as the amount of DEG increased, the size of TiO_2 crystallites slightly decreased. The crystallite size of anatase phase was decreased

from 21.10 nm without any DEG to 11.81 nm with the 1:2.0 mole ratio of TTiP:DEG. The results suggest that adding DEG reduces the crystallite size of TiO_2 nanoparticles. As a consequence, DEG is expected to have significant influence on photocatalytic activity due to the increased active surface area of the smaller size of nanoparticles.

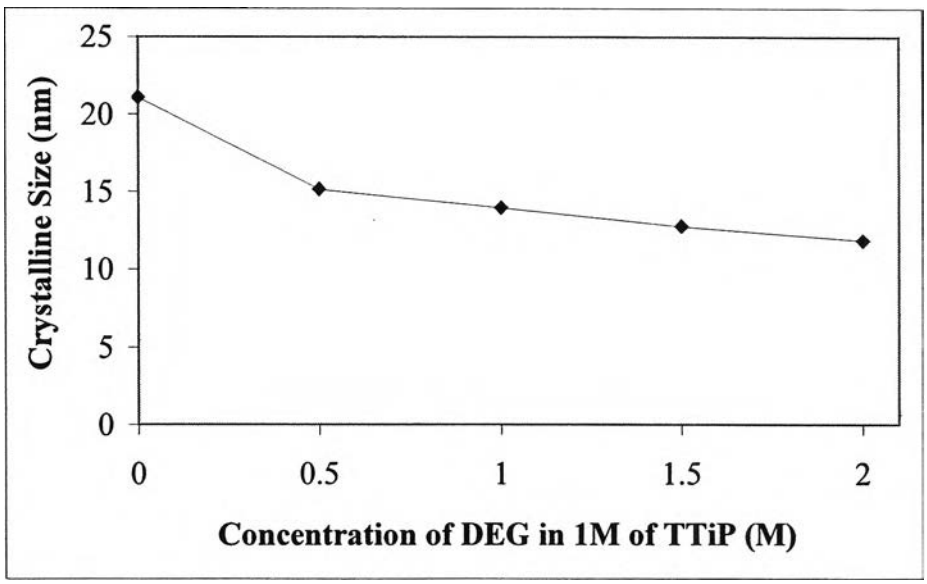

Figure 4.3 Nanocrystal size of TiO_2 with different mole ratios of DEG

The BET surface area of the synthesized TiO_2 was also determined and the results are shown in Figure 4.4. As discussed previously that DEG tends to decrease the crystalline size of TiO_2, this effect is confirmed by the measurement of surface area. If the crystalline size of TiO_2 decreases, the surface area of TiO_2 will be increased simultaneously. The effect of DEG on enhancing the surface area is clearly seen in Figure 4.4. Without any stabilizing agents, the surface area of crystalline size was 83.7 m^2/g. With the DEG addition to the preparation method with a ratio of TTiP:DEG as of 1:0.5, the surface area of TiO_2 became 176.87 m^2/g. Moreover, surface area of TiO_2 was gradually increased with the increasing of amount of DEG in the sol solution. Finally, the highest surface area of 205.76 m^2/g was obtained with the 1:2.0 TTiP:DEG.

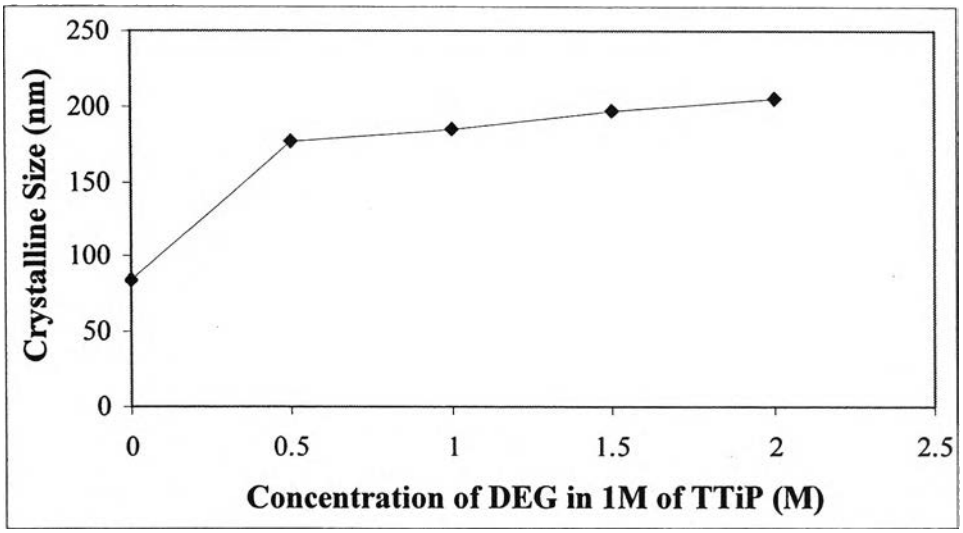

Figure 4.4 Surface area of the synthesized TiO_2 with different mole ratios of DEG

In terms of porosity of the sample set the pore volumes and the diameter of pores are shown in Table 4.2.

Table 4.2 Porosity of the synthesized TiO_2 with different mole ratios of DEG

Mole ratio of TTiP:DEG	Pore volume (cm^3/g)	Diameter of pore size (nm)
1:0	0.013	60.9
1:0.5	0.150	3.226
1:1.0	0.124	2.762
1:1.5	0.094	2.440
1:2.0	0.101	2.494

The effects of DEG on the pore volume and pore size are not drastic. With the small ratio of 1:0.5 TTiP:DEG, the pore volume and pore size were higher than at the higher ratio of 1:1.0 - 1:2.0. This observation may be due to the fact that, the major crystal phase of TiO_2 prepared by 1:0.5 TTiP:DEG was mostly anatase with a small amount of rutile. Due to the fact that the phase usually has larger crystal size, thus higher pore volume and size than the samples containing only anatase. For the conditions that only pure anatase formed, the addition of DEG does not have any significant effect on increasing the pore volume and the pore size.

4.1.1.2 Photocatalytic activity of nanocrystal TiO_2 with different mole ratios of DEG

To investigate the effect of nanocrystal TiO_2 preparing from different mole ratios of DEG on removal of hazardous wastes from the wastewater, the synthesized TiO_2 was used in the photocatalysis process of chromium (VI) removal from the synthetic wastewater.

In general, photocatalytic process involves different processes including adsorption–desorption, electron–hole pair production and recombination, and chemical conversion (Demeestere et al., 2004). Since recombination of photogenerated electron–hole pairs occurs within a fraction of a nanosecond, charge separation is only kinetically competitive if trapping species are already adsorbed prior to electron–hole pair generation (Fox and Dulay, 1993; Alberici and Jardim, 1997; Wittmann et al., 2005). In this work, the photocatalytic activity of nanocrystal TiO_2 is divided into two parts, adsorption and irradiation processes.

In adsorption process, the highest concentrations of adsorbed chromium (VI) on different types of TiO_2 surface were determined. Results of this experimental part are shown in Figure 4.5. It was found that the contact time to reach the equilibrium was 60 minutes. Apparently, the equilibrium concentrations of chromium (VI) in the aqueous solution using different types of TiO_2 were not significantly different. The adsorbed chromium (VI) was in the range of 0.692-1.109 mg Cr (VI)/g TiO_2. Adsorption data revealed that the 4.15-6.65% of the total amount of chromium (VI) in the reactor was adsorbed on the catalyst surface.

T 052019 80

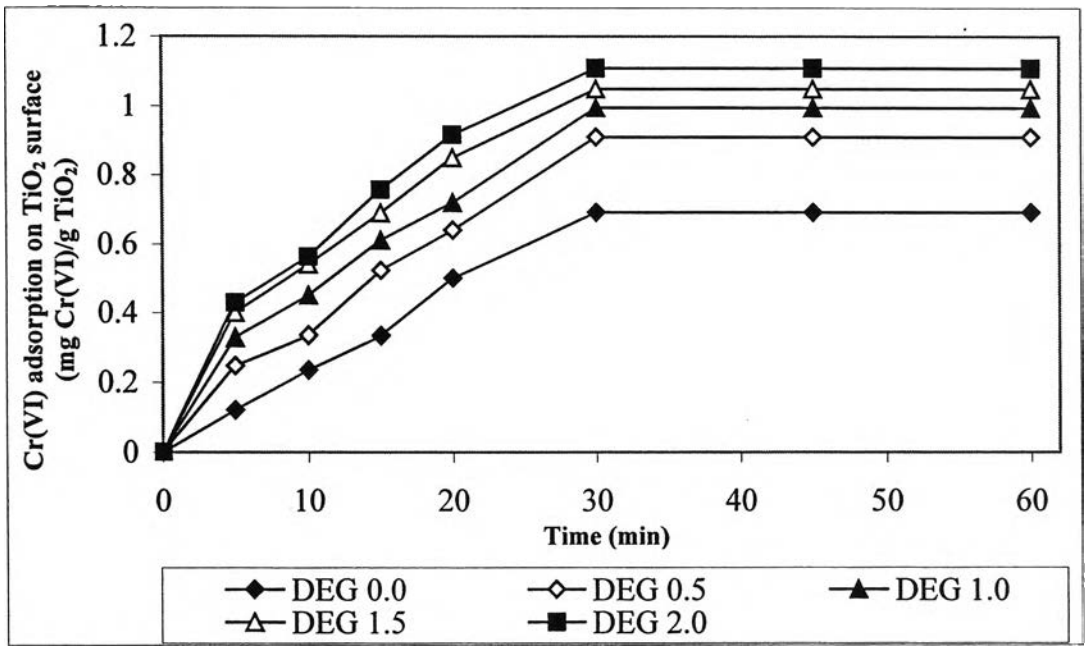

Figure 4.5 Adsorption of chromium (VI) on the surface of TiO_2 prepared with different mole ratios of TTiP:DEG

The photocatalytic reduction of chromium (VI) under irradiation process for the nanocrystal TiO_2 with different mole ratios of TTiP:DEG was compared. The ratio of residual to initial concentration of chromium (VI) in term of C/C_0 as a function of irradiation time was illustrated in Figure 4.6. It is obvious that the nanocrystal TiO_2 prepared without DEG provided the lowest efficiency in chromium (VI) removal compared to other conditions with some DEG. This might be due to the fact that TiO_2 prepared without DEG was a mixture of both anatase and rutile phases. When increasing amount of DEG, the rutile phase was not generated. Thus, with the pure anatase of TiO_2 synthesized by adding higher amount of DEG, the photocatalytic activity was much higher. However, as presented in the previous section, the nanoparticle size, pore volume, and pore size of the TiO_2 nanoparticles were not much different when TTiP:DEG was in the range of 1:1.0 - 1:2.0. Therefore, the photocatalytic activities obtained from these three conditions were not significantly different.

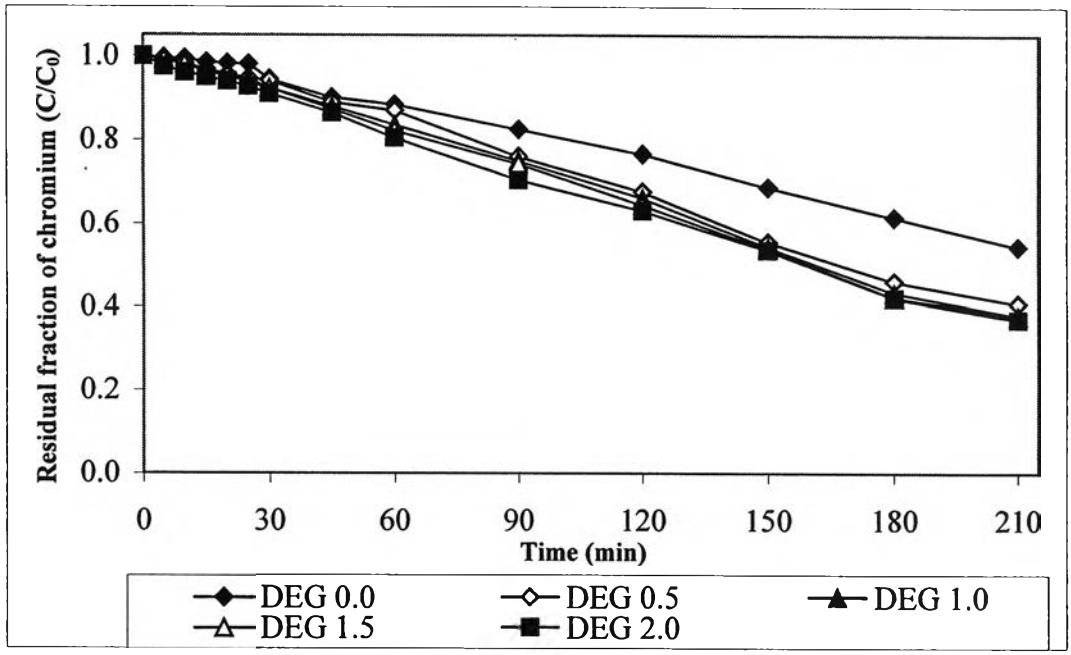

Figure 4.6 Photocatalytic reduction of chromium (VI) using different mole ratios of TTiP:DEG

To study the kinetic of the photocatalysis process, the observed kinetic constant, k_{obs}, from each experimental condition was also calculated. Considering the pattern of kinetic equation, the reaction behavior of nanocrystal TiO_2 in chromium (VI) removal was followed the zero-order pattern with the equations as follow:

$$\frac{dC}{dt} = -k[C]^0 = -k \tag{4.6}$$

$$dC = -k(dt) \tag{4.7}$$

$$\int_{C_0}^{C} dC = -k \int_{0}^{t} dt \tag{4.8}$$

$$C - C_0 = -k_{obs}t \tag{4.9}$$

where k_{obs} is the apparent reaction rate constant, t is the reaction time, C_0 is the initial concentration of chromium (VI) in aqueous solution, and C is the residual concentration of chromium (VI) at time t. The value of k_{obs} is determined by a linear regression method.

The plot of k_{obs} as a function of the amount of DEG presented in titania from each condition is shown in Figure 4.7. This figure shows that k_{obs} is dependent on the

amount of DEG. The values of k_{obs} and chromium (VI) removal efficiencies in each synthesis condition are also shown in Table 4.3. This behavior can be explained in terms of the surface area. The photocatalytic reaction is confined mostly to the surface of the TiO_2 nanoparticles under illumination. Therefore, the higher the surface area, the more the photocatalytic reaction occurs (Yoon et al., 2006) and the mole ratio of 1:2.0 TTiP:DEG provided the smallest size of nanocrystal TiO_2, highest surface area and porosity, the highest photocatalytic activity could be found at this condition.

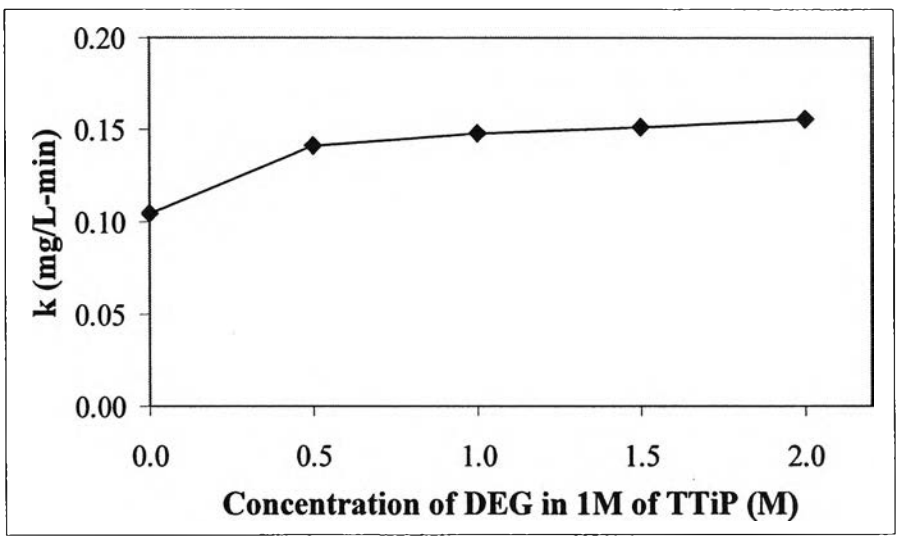

Figure 4.7 Comparison of photocatalytic decomposition rates using different mole ratios of TTiP:DEG

Table 4.3 Value of k_{obs} and chromium removal efficiencies of TiO_2 prepared from different mole ratios of TTiP:DEG

Mole ratio of TTiP:DEG	Equation	k	R^2	%Removal
1: 0.0	y = -0.1041x + 50	0.1041	0.9898	47.67
1: 0.5	y = -0.1411x + 50	0.1411	0.9909	61.37
1: 1.0	y = -0.1483x + 50	0.1483	0.9945	64.41
1:1.5	y = -0.1511x + 50	0.1511	0.9959	64.62
1: 2.0	y = -0.1551x + 50	0.1551	0.9976	65.20

4.1.2 Crystal growth of TiO_2 with DEG

4.1.2.1 Effect of calcination temperatures on nanocrystal TiO_2 prepared with DEG additive

As the amount of DEG in nanocrystal TiO_2 synthesis affects the TiO_2 properties, the grain growth pattern of TiO_2 with DEG stabilizing agents would be changed with the variation of calcination temperature. To study the effect of calcination temperature on nanocrystal TiO_2, the mole ratio of TTiP:DEG was fixed at 1:1.0 and the calcination time was 30 min, the calcination temperatures were varied as 300, 450, 500, 600, and 800 °C. A set of TiO_2 nanoparticles prepared without DEG was also calcined at the above temperatures for a comparison. The crystal structures of TiO_2 from each condition obtained from X-ray diffraction analysis are illustrated in Figure 4.8.

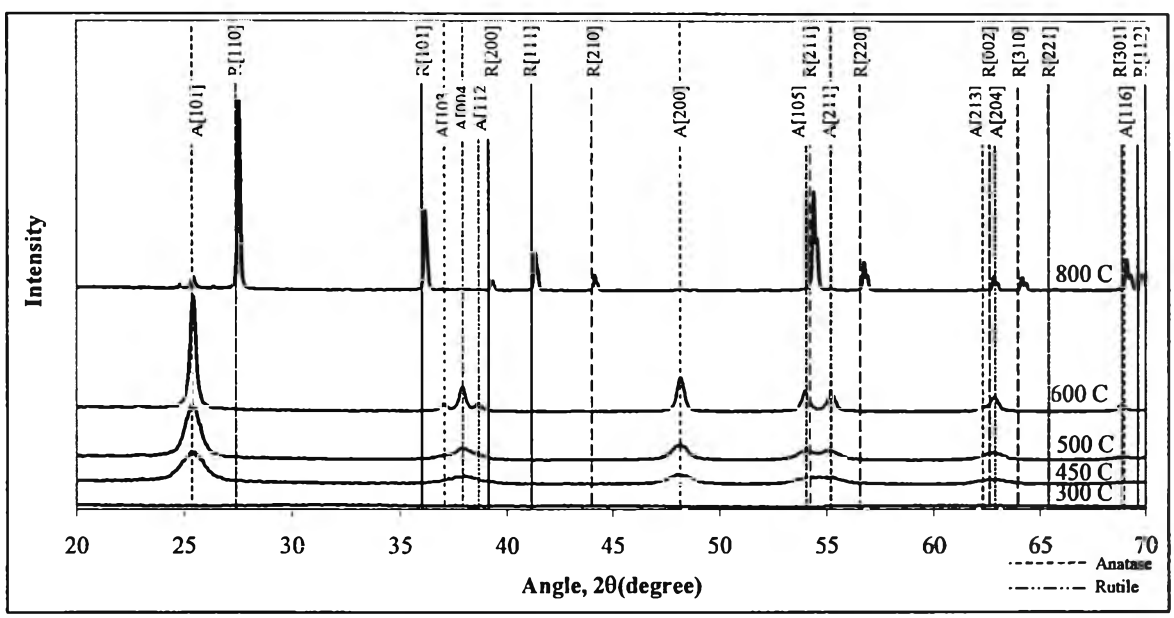

Figure 4.8 XRD patterns showing crystal structures of TiO_2 with 1:1.0 TTiP:DEG stabilizing agents at different calcination temperatures

As shown in Figure 4.8, anatase phase with a major peak corresponding to (1 0 1) was the predominant structure for the TiO_2 calcined at 300-600 °C. The growth of anatase was increased with the higher calcination temperature as shown in the figure. Rutile phase with a major peak corresponding to (1 1 0) was developed with the 800 °C calcination temperature while the intensity corresponding to the anatase phase was

reduced sharply. It is worth to note that the transformation of anatase to rutile phase of TiO_2 without DEG was developed at 450 °C.

Percentages of anatase and rutile phases were also calculated to compare the phase transformation of TiO_2 between TiO_2 synthesis with DEG stabilizing agents and without any stabilizing agents as shown in Table 4.4

Table 4.4 Percentages of anatase and rutile phases in samples obtained from different calcination temperatures

Calcination temperature (°C)	TiO_2 without stabilizing agents		TiO_2 with DEG	
	Anatase (%)	Rutile (%)	Anatase (%)	Rutile (%)
300 °C	100.00	0.00	100.00	0.00
450 °C	72.24	27.76	100.00	0.00
500 °C	42.02	57.98	100.00	0.00
600 °C	11.59	88.41	100.00	0.00
800 °C	0.00	100.00	5.52	94.48

From this experimental set, rutile phase in TiO_2 without any stabilizing agents was formed in lower calcination temperature than the TiO_2 with DEG. At the 500°C calcination temperature almost 60% of anatase phase in the TiO_2 without DEG has been transformed into rutile but no rutile phase was formed in the TiO_2 with DEG. With the same trend, at the 800 °C calcination temperature TiO_2 was completely formed in rutile phase in the TiO_2 without DEG but about 5.52 % of anatase phase was detected in the TiO_2 with DEG. It is suggested that DEG delays the transformation of anatase to rutile phase up to the calcination temperature of above 600°C.

The surface morphologies of TiO_2 nanocrystals from each condition are shown in Figure 4.9 (a)-(e). There is no obvious surface morphological difference with the different calcination temperatures in the range of 300-600°C However, when the calcination temperature increased to 800°C, the size of nanocrystal TiO_2 was significant bigger than those obtained from the lower calcination temperatures.

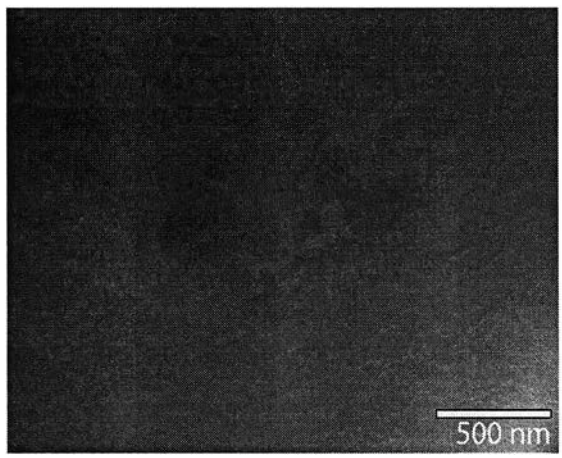

(a) TiO_2 calcined at 300 °C

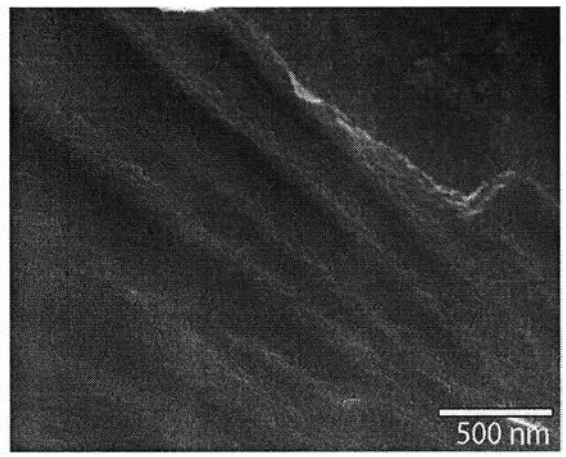

(b) TiO_2 calcined at 450 °C

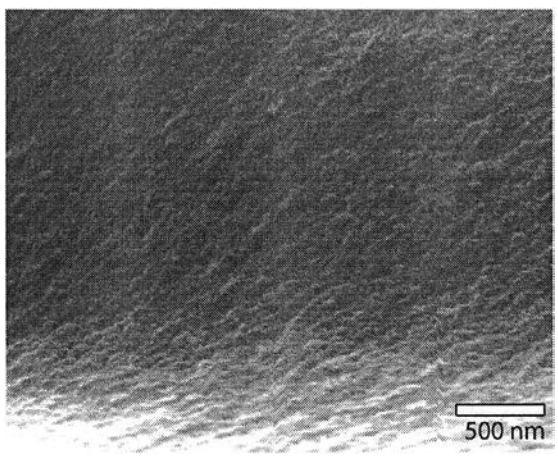

(c) TiO_2 calcined at 500 °C

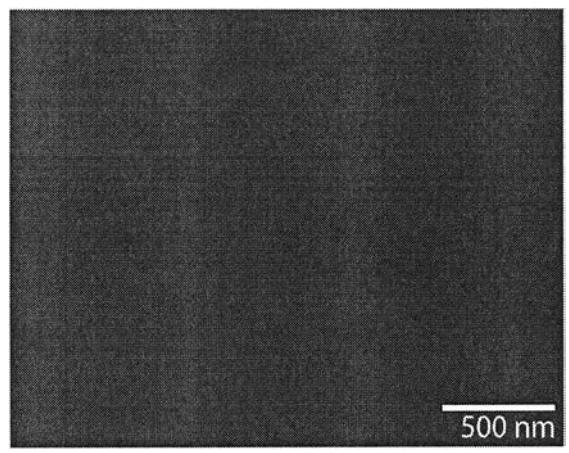

(d) TiO_2 calcined at 600 °C

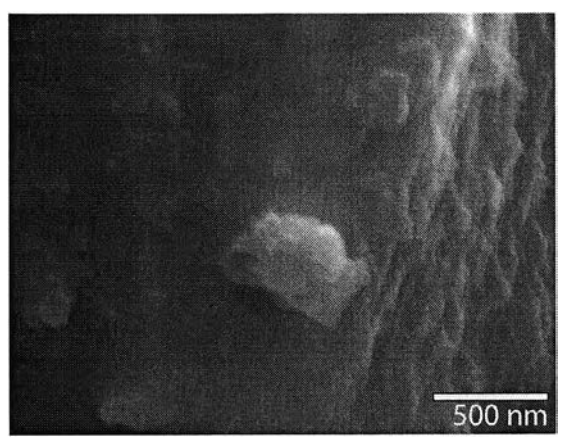

(e) TiO_2 calcined at 800 °C

Figure 4.9 SEM images showing surface morphology of TiO_2 nanocrystal with DEG in different calcination temperatures

To determine that growth of nanocrystal TiO_2 is dependent on the calcination temperature, the sizes of nanocrystal TiO_2 from each condition were calculated using Debye-Scherrer equation. Summary of size variation of TiO_2 nanocrystal synthesized with DEG stabilizing agent and the calcination temperatures is shown in Table 4.5. The size variation of TiO_2 nanocrystal synthesized without any stabilizing agents is also included in the same table for comparison.

Table 4.5 Sizes of anatase and rutile of TiO_2 in samples prepared at different calcination temperatures

Calcination temperature (°C)	**TiO_2 without stabilizing agents**		**TiO_2 with DEG**	
	Anatase (nm)	**Rutile (nm)**	**Anatase (nm)**	**Rutile (nm)**
300 °C	9.31	-	-	-
450 °C	21.10	37.45	13.88	-
500 °C	31.03	56.18	20.82	-
600 °C	39.57	76.24	32.97	-
800 °C	-	76.24	83.30	164.21

As shown in the table, the particle size increases with increasing calcination temperature. The particles grow slowly at low calcination temperatures and then becomes very fast at high calcination temperatures. The relationship between the particle size and the calcination temperatures in reported here is in agreement with the results reported in previous works (Sullivan and Cole, 1959; Li et al., 2002). This behavior can be explained by the equation (Turnbull, 1956)

$$u = a_0 \nu_0 \left[\exp\left(-\frac{Q}{KT} \right) \right] \tag{4.10}$$

where u is the growth rate, a_0 is the particle diameter, ν_0 the atomic jump frequency, Q the activation energy for an atom to leave the matrix and attach itself to the growing phase, and T is the calcination temperature.

When the calcination temperature is high, the activation energy is very small and the growth rate is large. Thus, the particle size increases very quickly as the

calcination temperature increases. In contrast, when the calcination temperature is low, the activation energy is very large and the growth rate becomes slow. Therefore, the grain size increases very slowly as the calcination temperature increases (Li et al., 2002).

Considering the DEG effect on grain growth of TiO_2, it was found that, in average, size of nanocrystal TiO_2 with DEG addition was smaller than those without stabilizing agents. It is worth to note that the grain size of anatase is normally smaller than the rutile. As discussed previously, when the calcination temperature is lower than 800°C, the phase of TiO_2 with DEG was fully anatase, while phase of TiO_2 without any stabilizing agents contained both anatase and rutile. This difference in phase of TiO_2 is expected to be the cause of the difference in the properties of nanosize TiO_2.

At the calcination temperature of 300 °C, nanosizes of TiO_2 without any stabilizing agents were about 9.31 nm, and the phase is completely anatase. Above 450°C, growth of TiO_2 was observed due to the transformation of anatase to rutile phase. For rutile, the crystal size was increased drastically from 37.45 nm at 450°C to 56.18 nm at 600 °C and the crystal size of anatase was also increased from 21.10 nm at 450°C to 39.57 nm at 600 °C. Above 600 °C, the nanocrystal size of titania was 76.24 nm which was mostly by rutile phase. At the selected calcination temperature in the range of 450-600 °C, it is found that the nanocrystal size of TiO_2 with DEG was relatively smaller than that of TiO_2 synthesized without any stabilizing agents. This is due to the fact that the TiO_2 with DEG was mostly or completely anatase phase.

Table 4.6 shows the surface area of TiO_2 prepared from the range of above calcination temperatures. It can be clearly seen that, when comparing the surface areas of TiO_2 without any stabilizing agents and TiO_2 with DEG, DEG not only decreases the size of nanoparticles but also increases the surface area of nanoparticles. When varying calcination temperature, the surface area of TiO_2 was drastically changed. As calcination temperature increased, the size of nanoparticle increases resulting in the reduced surface area. Moreover, the calcination temperature leads to the phase transformation from anatase to rutile yielding the increasing of pore diameter with the exception when TiO_2 is in the amorphous phase, which was formed at 300 °C calcination temperature.

Table 4.6 Surface area and pore diameter of TiO_2 at different calcination temperatures

Calcination temperature (°C)	TiO_2 without DEG		TiO_2 with DEG	
	Surface area (m^2/g)	Pore diameter (nm)	Surface area (m^2/g)	Pore diameter (nm)
300 °C	174.50	2.285	1.63	9.391
450 °C	83.73	5.981	185.30	2.763
500 °C	22.20	5.914	82.25	4.362
600 °C	0.52	17.830	4.23	8.055
800 °C	0.43	12.670	3.11	15.250

4.1.2.2 Photocatalytic activity of nanocrystal TiO_2 prepared with DEG at different calcination temperatures

Effects of calcination temperature on photocatalytic activity of nanocrystal TiO_2 were studied. In this experimental set, TiO_2 nanopowders obtained previously at calcination temperatures in the range of 300 °C to 600 °C were used and the amount of TiO_2 in each study was fixed at 3 g/L. The experiments in this section were divided into two parts, adsorption and irradiation process.

The highest concentrations of adsorbed chromium (VI) on TiO_2 surface using different types of TiO_2 in adsorption process were determined and shown in Figure 4.10. The photocatalytic reduction of chromium (VI) under irradiation process for the nanocrystal TiO_2 with different molar ratios of TTiP:DEG was also compared and the ratio of residual to initial concentration of chromium (VI) in terms of C/C_0 as a function of irradiation time was illustrated in Figure 4.11. It was found that the contact time to reach the equilibrium was 60 minutes. The equilibrium concentrations of chromium (VI) in the aqueous solution using different types of TiO_2 were considerably different. The adsorbed chromium (VI) was in the range of 0.343-1.0 mg Cr(VI)/g TiO_2. Adsorption data revealed that the 2.06-5.97% of the total amount of chromium (VI) in the reactor was adsorbed on the catalyst surface. Generally, the major factor affecting the adsorption process is surface area of TiO_2. Thus, since the TiO_2 from 450 °C calcination temperature provided the smallest size of 13.88 nm and the highest surface area of 185.30 m^2/g, the TiO_2 from this condition can attract the highest amount of chromium (VI) on the particle surface.

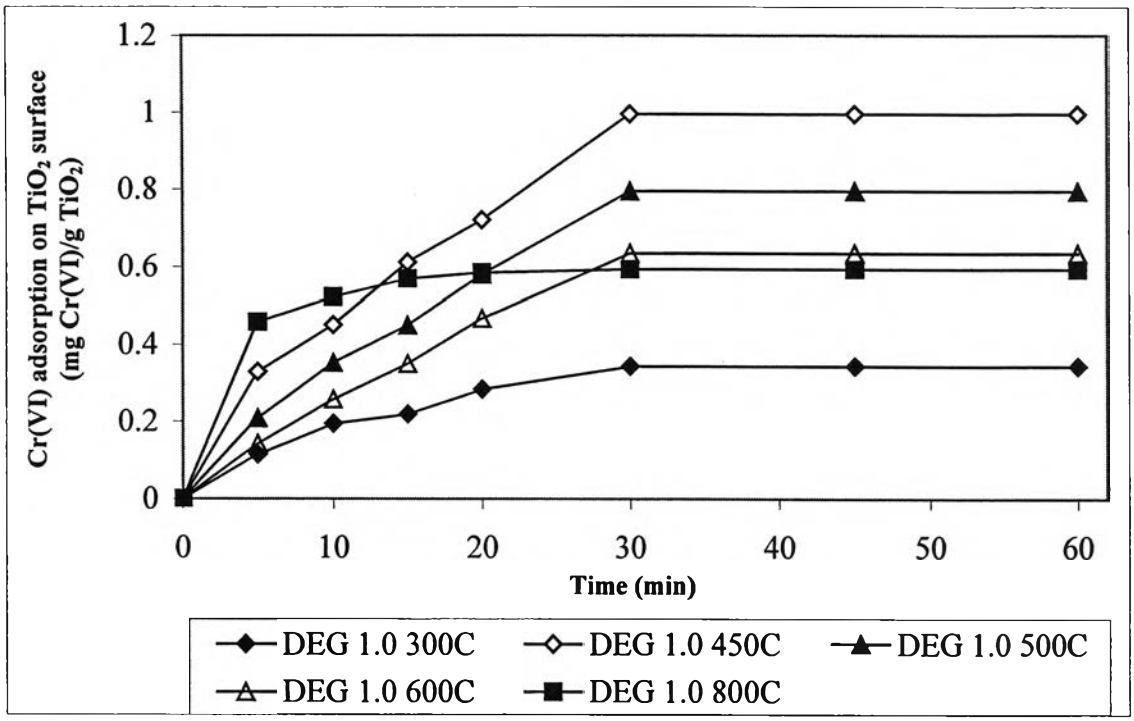

Figure 4.10 Adsorption of chromium (VI) on the surface of TiO_2 prepared at different calcination temperatures as a function of time

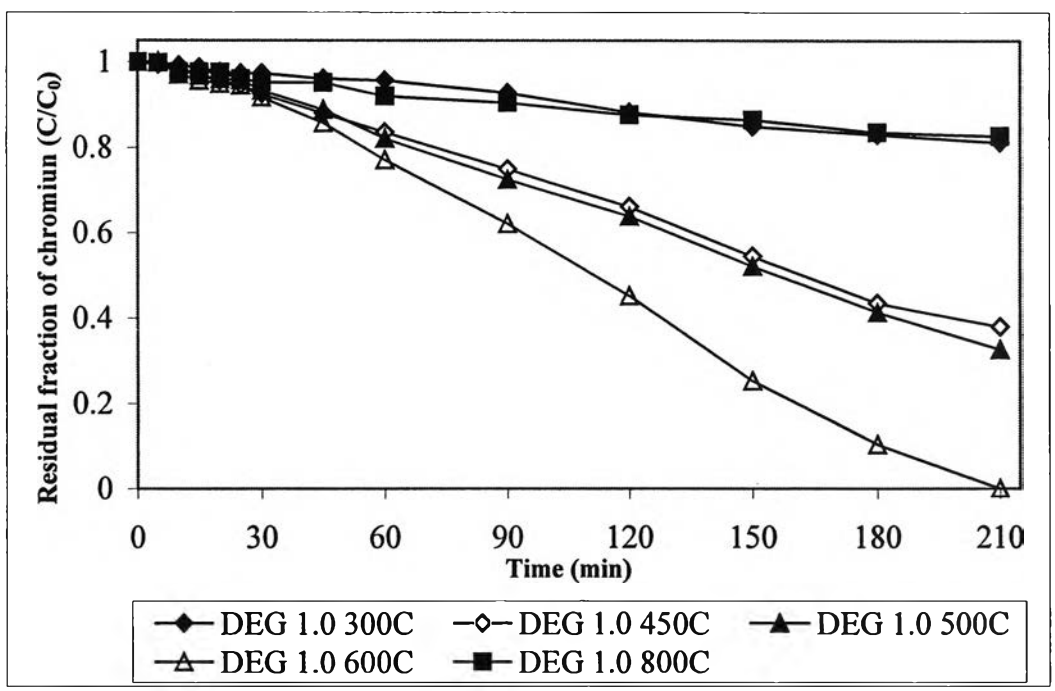

Figure 4.11 Photocatalytic reduction of chromium (VI) by TiO_2 prepared at different calcination temperatures as a function of time

สำนักงานวิทยทรัพยากร จุฬาลงกรณ์มหาวิทยาลัย

It is obvious that the nanocrystal TiO_2 prepared at 600°C calcination temperature provided the highest efficiency in chromium (VI) removal compared to other conditions. It is worth to note that the TiO_2 with 450°C calcination temperature provided the highest amount of chromium (VI) adsorption on titania surface, while the TiO_2 with 600°C calcination temperature provided the highest amount of chromium (VI) reduction upon irradiation process. This may be due to the fact that crystal phase of TiO_2 at the 600 °C calcination temperature was pure anatase phase with highest amount of TiO_2 in the crystal compare to those obtained from other calcination temperatures as shown by XRD pattern in Figure 4.8. In addition, the pore diameter of TiO_2 in this condition was the largest (80.5 Å) compared to those obtained from other conditions having the pure anatase.

In terms of kinetics, the photocatalytic reduction reactions of chromium (VI) of nanocrystal TiO_2 obtained from various calcination temperatures were followed the zero-order pattern. The values of k_{obs} were calculated and the plots of k_{obs} as a function of calcination temperature are shown in Figure 4.12. This figure shows that k_{obs} increased with increasing calcination temperatures. However after reached the highest value for sample of 600 °C calcination temperature, the value of k_{obs} decreased. From this information, the photocatalytic activity as represented by the k_{obs} was mainly governed by the anatase phase of TiO_2. As the amount of anatase TiO_2 increased with calcination temperature, the photocatalytic activity increased. At calcination temperature higher than 600 °C, crystal phase was transformed to rutile, causing the decreased of photocatalytic activity. For the effect of nanocrystal size of TiO_2, it was found that nanocrystal size has less effect than the titania crystal phase as the value of nanocrystal size is slightly difference in the range of 13-33 nm for the range of calcination temperature. It is worth to note that in the photocatalysis process, the photocatalytic oxidation-reduction process during irradiation is much more the major mechanism in contaminant removal than the adsorption process at the beginning step. Thus, in overall consideration, the TiO_2 with 600 °C calcination temperature provided the best condition for chromium (VI) removal.

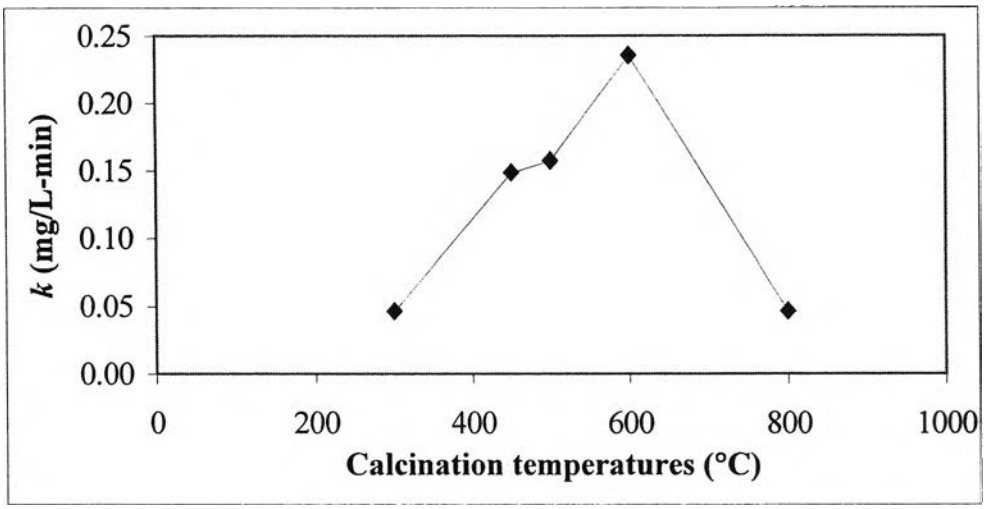

Figure 4.12 Comparison of photocatalytic decomposition rates using different calcination temperature

4.1.3 Determination of adsorption isotherm of TiO_2 with DEG as additive

To obtain the adsorption characteristics of TiO_2 with DEG, it is necessary to determine the adsorption isotherm of the titania. The best condition from the previous section (TTiP:DEG mole ratio = 1:1, and 600 °C calcination temperature) is used in this part. The adsorption of chromium (VI) with TiO_2 as the initial concentration of chromium (VI) varied in the range of 10-100 mg/L was conducted. The results of this experimental part are shown in Figure 4.13. It is obvious that the amount of chromium (VI) adsorbed on titania surface is increased with increasing initial concentration of chromium (VI) in the water.

To obtain the adsorption isotherm of TiO_2, the plot of adsorbed chromium (VI) on titania surface (mg Cr(VI)/mgTiO_2) versus the concentration of chromium (VI) in the solution after reaching the equilibrium (mg/L) was performed as shown in Figure 4.14. The value of adsorbed chromium (VI) on titania surface was increased with increasing of the equilibrium concentration of chromium (VI) until it reached the certain value and the plateau of the adsorption pattern was obtained.

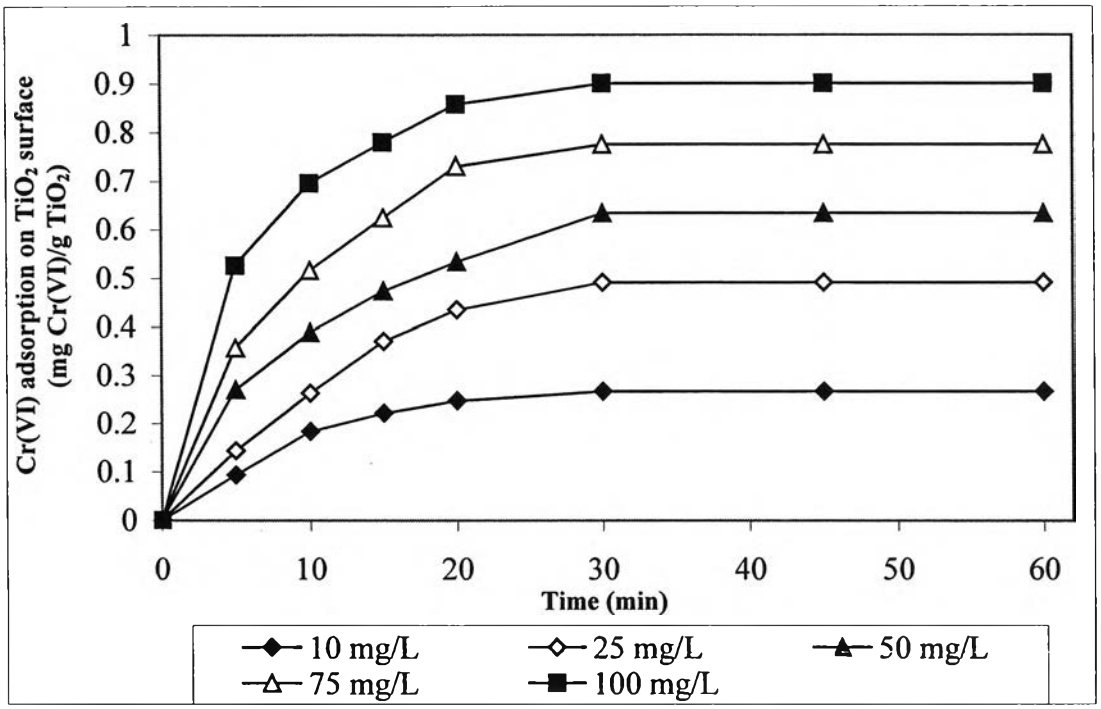

Figure 4.13 Adsorption of chromium (VI) on the surface of TiO_2 at different initial concentration of chromium (VI) as a function of time

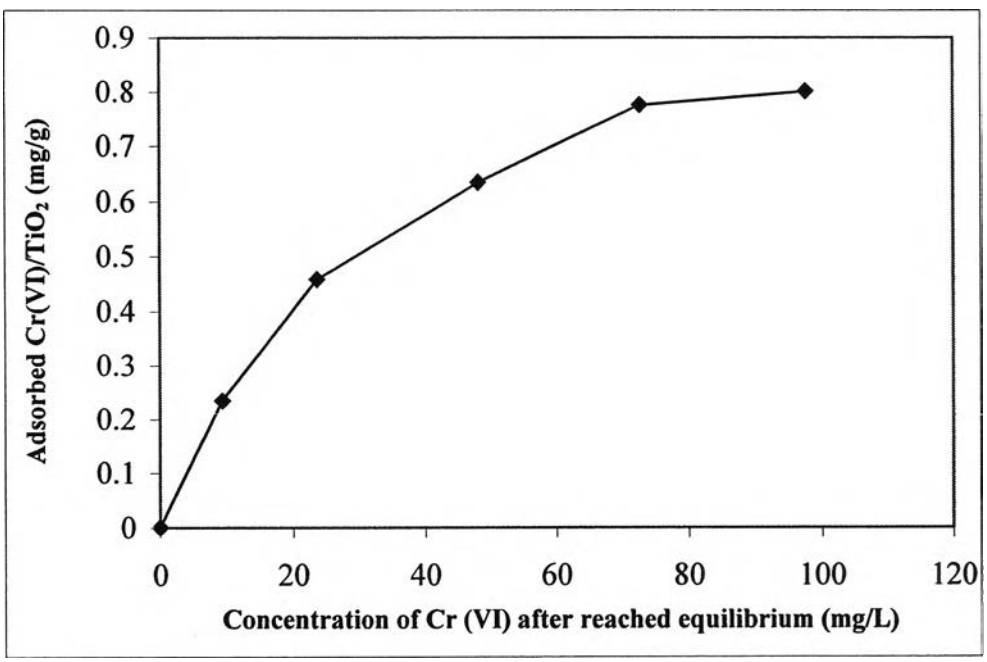

Figure 4.14 Plot of Cr (VI) equilibrium concentration vs. chromium (VI) adsorbed concentration on TiO_2 surface

The values of chromium (VI) adsorption at the equilibrium condition were used further in determining the adsorption isotherm in both Langmuir and Freundlich equations.

The Langmuir equation was applied for the adsorption equilibrium of chromium (VI) onto TiO_2 surfaces. The Langmuir adsorption isotherm is based on these assumptions: (i) maximum adsorption corresponds to a saturated monolayer of adsorbate molecules on the adsorbent surface; (ii) the energy of adsorption is constant; and (iii) there is no transmigration of adsorbate in the surface plane. The Langmuir equation is shown below:

$$\frac{C_e}{(x/m)} = \frac{1}{(Q_0 b)} + \frac{C_e}{Q_0} \qquad (4.11)$$

where C_e is the equilibrium concentration of chromium (VI), mg/L, *(x/m)* is the amount of adsorbed chromium (VI) at equilibrium per unit mass of TiO_2, mg/g, and Q_0 and b are Langmuir constants related to adsorptive capacity and energy of adsorption, respectively.

The linear plot of $C_e/(x/m)$ vs. C_e in Figure 4.15 shows that the adsorption of chromium (VI) onto the TiO_2 surface obeys the Langmuir adsorption isotherm.

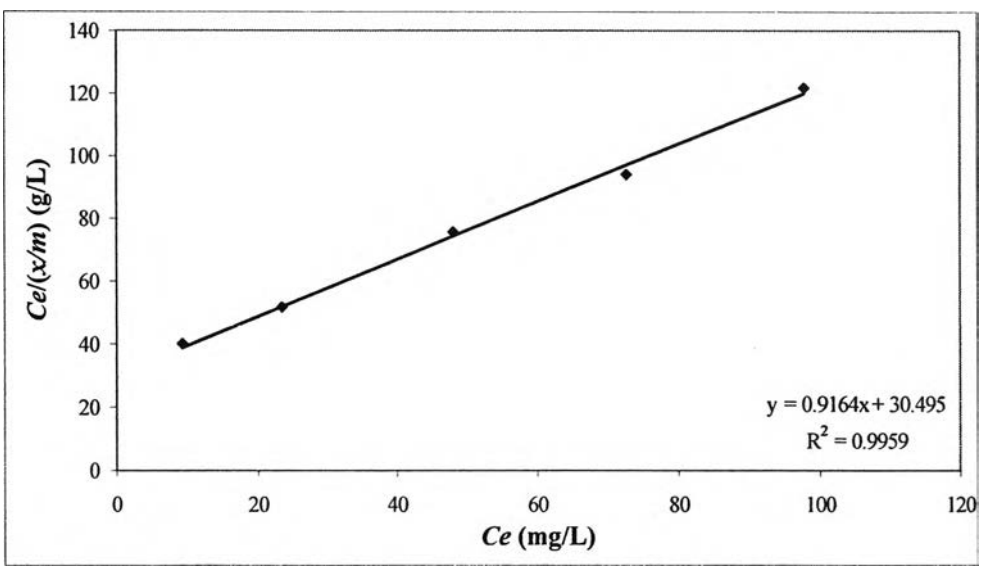

Figure 4.15 Langmuir adsorption isotherm plots
for the adsorption of chromium (VI) onto the TiO_2 surface

The correlation coefficient for the linear regression fit of the Langmuir plot was found to be 0.9959. The equation 4.11 becomes:

$$\frac{C_e}{(x/m)} = 0.9164C_e + 30.495 \qquad (4.12)$$

The Langmuir constants Q_0 and b were determined from the Langmuir plots and found to be 1.09 mg/g and 0.030 L/mg respectively.

The essential characteristic of the Langmuir isotherm can be expressed in term of a dimensionless constant separation factor or equilibrium parameter, R_L, which is defined by (Mckay et al., 1982)

$$R_L = 1/(1+bC_0) \qquad (4.13)$$

where b is the Langmuir constant, and C_0 is the initial concentration of chromium (VI). R_L values and the corresponding behavior are summarized in Table 4.7. The calculated values of R_L in this experiment set were shown in Table 4.8 and it was found that all values are between 0 and 1, indicating favorable chromium (VI) adsorption onto the TiO_2 surface.

Table 4.7 R_L Value and Isotherms

R_L Value	**Behavior of isotherm**
$R_L > 1$	Unfavorable
$0 < R_L < 1$	Favorable
$R_L = 0$	Irreversible

Table 4.8 Value of R_L for Langmuir adsorption isotherm for TiO_2 with DEG

Initial concentration of chromium (VI) (mg/L)	**R_L Value**
10	0.77
25	0.58
50	0.41
75	0.31
100	0.26

The Freundlich equation was also applied to describe the adsorption of chromium (VI) onto the TiO_2 surface. The Freundlich equation is basically empirical, and generally agrees with the experimental data over a moderate range of adsorbate concentrations. The Freundlich isotherm is represented by the equation (Mckay et al., 1982)

$$\log(x/m) = (1/n)\log C_e + \log k_f \qquad (4.14)$$

where C_e is the equilibrium concentration of chromium (VI), mg/L, *(x/m)* is the amount of adsorbed chromium (VI) at equilibrium per unit mass of TiO_2, mg/g, and k_f and n are the Freundlich constants.

The linear plot of log *(x/m)* vs. log C_e in Figure 4.16 shows that the adsorption of chromium (VI) onto the TiO_2 surface obeys the Freundlich adsorption isotherm.

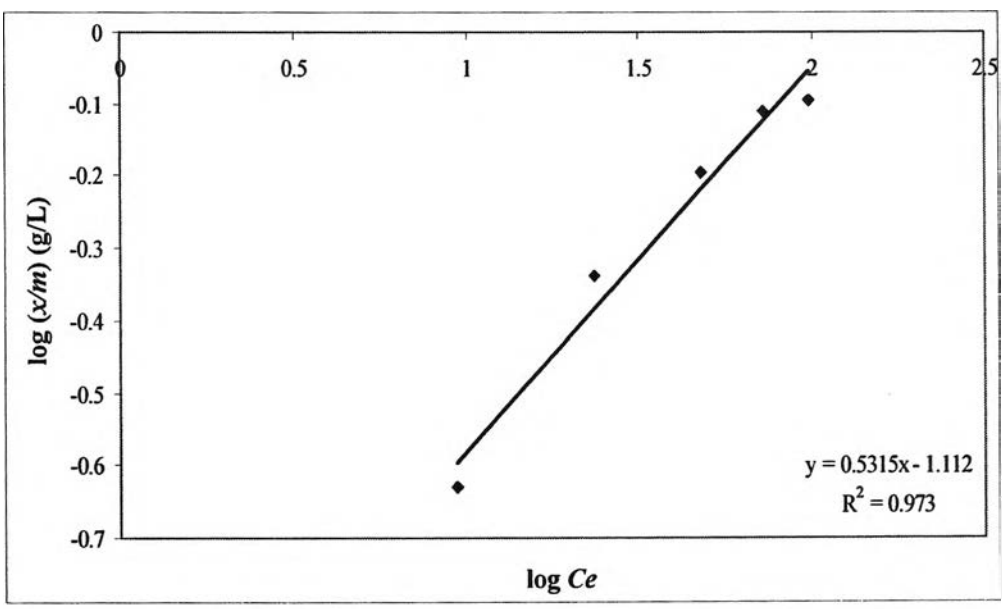

Figure 4.16 Freundlich adsorption isotherm plots for the adsorption of chromium (VI) onto TiO_2 surface

The expressed equation is

$$\log(x/m) = 0.5315\log C_e - 1.112 \qquad (4.15)$$

The correlation coefficient for the Freundlich plot was found to be 0.9730, which was less than that from the Langmuir plot. The value of correlation coefficient of chromium (VI) adsorption indicates that the adsorption behavior of chromium (VI) onto TiO_2 tends to be a monolayer adsorption as described by the Langmuir isotherm rather than the Freundlich isotherm.

4.1.4 Determination of kinetic values following Langmuir-Hinshelwood Model for TiO_2 with DEG as stabilizing agent

Additional kinetic values were obtained using Langmuir-Hinshelwood model. The best condition from the previous section (TTiP:DEG mole ratio = 1:1, and 600 °C calcination temperature) was used in this part. The photocatalytic reduction of chromium (VI) by TiO_2 with variation of initial concentration of chromium (VI) in the range of 10-100 mg/L was conducted.

The results of this experimental part are shown in Figure 4.17. It is obvious that the efficiency in chromium (VI) removal decreased with the increasing of initial concentration of chromium (VI) in the water. To explain the behavior of photocatalytic reduction of chromium (VI) by the synthesized TiO_2 in term of kinetic study, two patterns of kinetic orders, which are zero-order and pseudo-first order equations, are considered. As can be seen in the chromium (VI) declining pattern, the kinetic order to explain the existing reaction can be either zero-order or pseudo first order. Thus, the value of k_{obs} can be calculated by both equations.

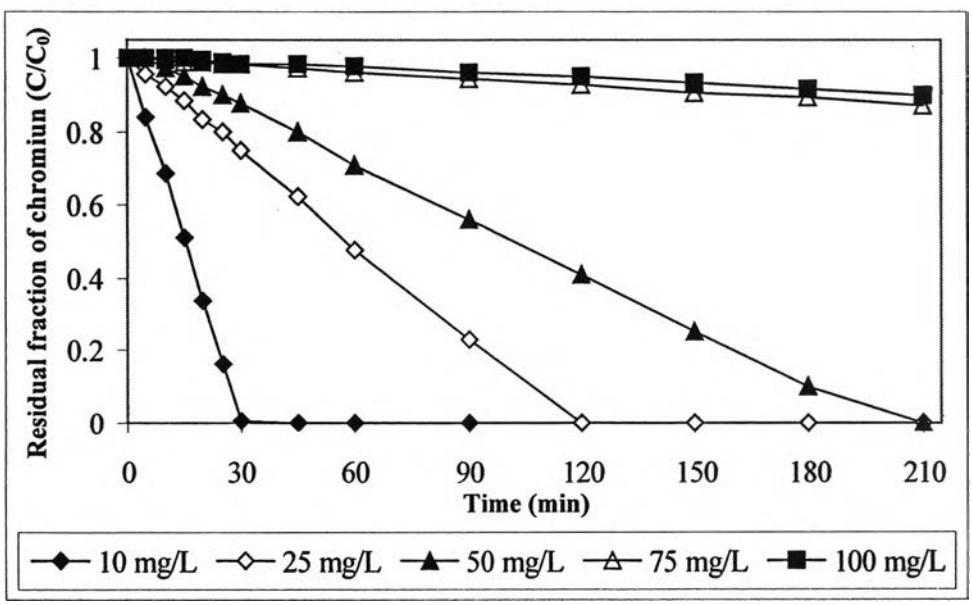

Figure 4.17 Photocatalytic reduction of chromium (VI) as a function of time using different initial concentration of chromium (VI)

The zero-order equation can be derived as follow:

$$\frac{dC}{dt} = -k[C]^0 = -k \tag{4.16}$$

$$dC = -k(dt) \tag{4.17}$$

$$\int_{C_0}^{C} dC = -k \int_{0}^{t} dt \tag{4.18}$$

$$C - C_0 = -k_{obs}t \tag{4.19}$$

where k_{obs} is the apparent reaction rate constant, t is the reaction time, C_0 is the initial concentration of chromium (VI) in aqueous solution, and C is the residual concentration of chromium (VI) at time t. Value of k_{obs} was determined from the slope of graph which was plotted between C-C_0 and reaction time, t. The value R^2 for linear regression was calculated to exhibit the tendency of the reaction pattern to be a zero-order pattern. Values of k_{obs} from zero-order equation were determined as shown in Table 4.9.

The pseudo-first order equation can be obtained by the following relationship of C and t:

$$\frac{d[C]}{dt} = -k_{obs}[C]^n = -k_{obs}[C]^1 \tag{4.20}$$

$$\frac{1}{[C]}d[C] = -k_{obs}dt \tag{4.21}$$

$$\int_{C_0}^{C} \frac{1}{[C]}d[C] = -\int_{0}^{t} k_{obs}dt \tag{4.22}$$

$$\ln(\frac{C}{C_0}) = -k_{obs}t \tag{4.23}$$

where k_{obs} is the apparent reaction rate constant, t is the reaction time, C_0 is the initial concentration of chromium (VI) in aqueous solution, and C is the residual concentration of chromium (VI) at time t. Value of k_{obs} was determined from the slope of graph which was plotted between $-ln\ (C/C_0)$ and reaction time, t. The value R^2 for linear regression was calculated to exhibit the tendency of the reaction pattern to be a

pseudo-first order pattern. Values of k_{obs} from pseudo-first order equation were determined as shown in Table 4.10.

Table 4.9 Values of k_{obs} from zero-order equation for photocatalytic process using TiO_2 with DEG for chromium (VI) removal

Initial concentration of chromium (VI) (mg/L)	k_{obs} **(mg/L-min)**	R^2	**% Removal**	**Final concentration of chromium (VI) (mg/L)**
10	0.3310	0.9994	100.00	0.00
25	0.3049	0.9482	100.00	0.00
50	0.2432	0.9975	100.00	0.00
75	0.0592	0.9848	14.62	64.03
100	0.0481	0.9388	11.10	88.90

Table 4.10 Values of k_{obs} from pseudo-first order equation for photocatalytic process using TiO_2 with DEG for chromium (VI) removal

Initial concentration of chromium (VI) (mg/L)	k_{obs} **(min^{-1})**	R^2	**% Removal**	**Final concentration of chromium (VI) (mg/L)**
10	0.05930	0.8997	100.00	0.00
25	0.02030	0.9370	100.00	0.00
50	0.00920	0.8480	100.00	0.00
75	0.0022	0.9903	44.39	41.71
100	0.0016	0.9933	30.23	69.77

Considering the pattern of kinetic equation, the photocatalytic reduction reactions of chromium (VI) by TiO_2 with DEG can be represented by zero-order pattern when initial concentration was relatively low in the range of 10-50 mg/L. However, as concentration of chromium (VI) was leveled up, the kinetic pattern was changed from the zero-order pattern to the first-order pattern as represented by the R^2 values. The change of the reaction behavior can be explained that at low level of chromium (VI) concentration, the reaction was dependent only on the reaction time and it was independent from the concentration of chromium (VI) in the aqueous

solution. The surface of titania is not the limitation of the reaction. As chromium (VI) concentration increased with the fixed dosage of TiO_2 in the system, the reaction became dependent on both concentration of chromium (VI) and the reaction time. Results from this experiment set provide the important information that at low level of contaminant concentration, the reaction can be described by zero-order pattern and at high level of contaminant concentration, the reaction is best described by pseudo first-order pattern.

The value of k_{obs} obtained from the pseudo first-order pattern can be used further to find the intrinsic kinetic coefficient occurred during irradiation process of photocatalysis. The intrinsic kinetic values of photocatalysis can be determined from the Langmuir-Hinshelwood model. In this model, the reaction rate for second-order surface decomposition of chromium (VI) can be represented as:

$$rate = -\frac{d[Cr]}{dt} = k_c \frac{K_{Cr}[Cr]}{1 + K_{Cr}[Cr]_0} \tag{4.24}$$

where $[Cr]$ is the Cr concentration at time t,

k_c is the second-order rate constant,

K_{Cr} is the equilibrium adsorption constants of chromium (VI) onto TiO_2, and

$[Cr]_0$ is the initial concentration of chromium (VI)

The photocatalytic degradation of chromium (VI) in the presence of TiO_2 exhibits pseudo first-order kinetics with respect to chromium (VI) concentration as in

$$-\frac{d[Cr]}{dt} = k_{obs}[Cr] = k_c \frac{K_{Cr}}{1 + K_{Cr}[Cr]_0}[Cr] \tag{4.25}$$

where k_{obs} is the observed pseudo first-order rate concentration for the photocatalytic reduction of chromium (VI). Therefore, the integration of Equation (4.25) results in

$$\ln\left(\frac{[Cr]_0}{[Cr]}\right) = k_{obs}t \tag{4.26}$$

Based on Equation (4.26), the straight-line relationship of $ln([Cr]_0/[Cr])$ versus irradiation time, t, was obtained as listed in Table 4.11.

Next, the relationship between k_{obs} and $[Cr]_0$ from Eq. (4.25) can be expressed with Equation (4.27)

$$\frac{1}{k_{obs}} = \frac{1}{k_c K_{Cr}} + \frac{[Cr]_0}{k_c} \tag{4.27}$$

Equation (4.27) shows that the linear expression also can be obtained by plotting the reciprocal of degradation rate $(1/k_{obs})$ as a function of the initial chromium (VI) concentration.

To obtain a kinetic value for both k_c and K_{cr}, the experiment with initial chromium (VI) concentration as of 60, 70, 80, and 90 mg/L were added. The values of k_{obs} from pseudo-first order equation were calculated and shown in Table 4.11.

Table 4.11 Values of k_{obs} used in Langmuir-Hinshelwood model for photocatalytic process using TiO_2 with DEG for chromium (VI) removal

Initial concentration of chromium (VI) (mg/L)	k_{obs} **(min^{-1})**	R^2	**% Removal**	**Final concentration of chromium (VI) (mg/L)**
60	0.0025	0.9789	40.84	35.49
70	0.0024	0.9899	39.59	42.29
75	0.0022	0.9803	44.39	41.71
80	0.0020	0.9820	34.30	52.56
90	0.0018	0.9910	31.48	61.67
100	0.0016	0.9833	30.23	69.77

Figure 4.18 shows that the linear expression also can be obtained by plotting the reciprocal of degradation rate $(1/k_{obs})$ as a function of the initial chromium (VI) concentration. By means of a least square best fitting procedure, the values of the adsorption equilibrium constant (K_{Cr}), and the second-order rate constant (k_c) were obtained, and this value found to be K_{Cr} = 0.287 L/mg and k_c = 0.168 mg/L-min (R^2 = 0.9687), respectively.

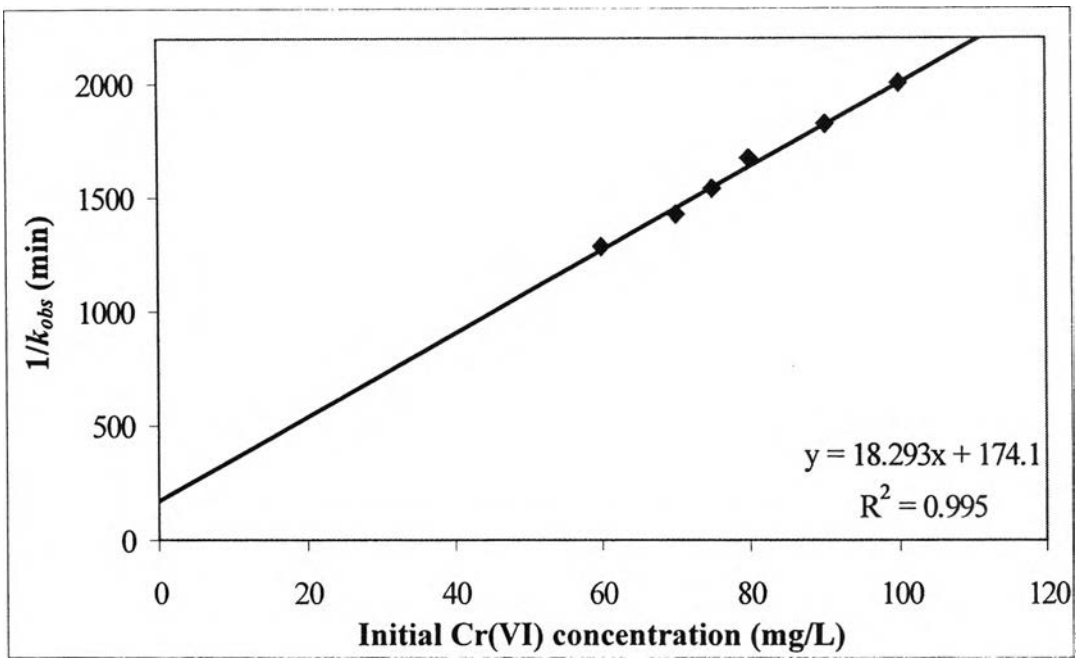

Figure 4.18 Photocatalytic reduction of chromium (VI) using TiO_2 with DEG

4.2 Effect of PEG stabilizing agent

4.2.1 Formation of crystal with PEG

4.2.1.1 Formation of crystal with different molar ratios of PEG

In this work, to investigate the effect of PEG on the formation of nanocrystal TiO_2, the different mole ratios of PEG were varied. However, the calcination temperature was kept constant at 450 °C. The mole ratios of TTiP:PEG included 1:0, 1:0.5:, 1:1. 1:1.5, and 1:2.0. The crystal structures of TiO_2 from each condition obtaining from X-ray diffraction analysis are illustrated in Figure 4.19 and the corresponding surface morphology of TiO_2 nanocrystals are shown in Figures 4.20 (a)-(e).

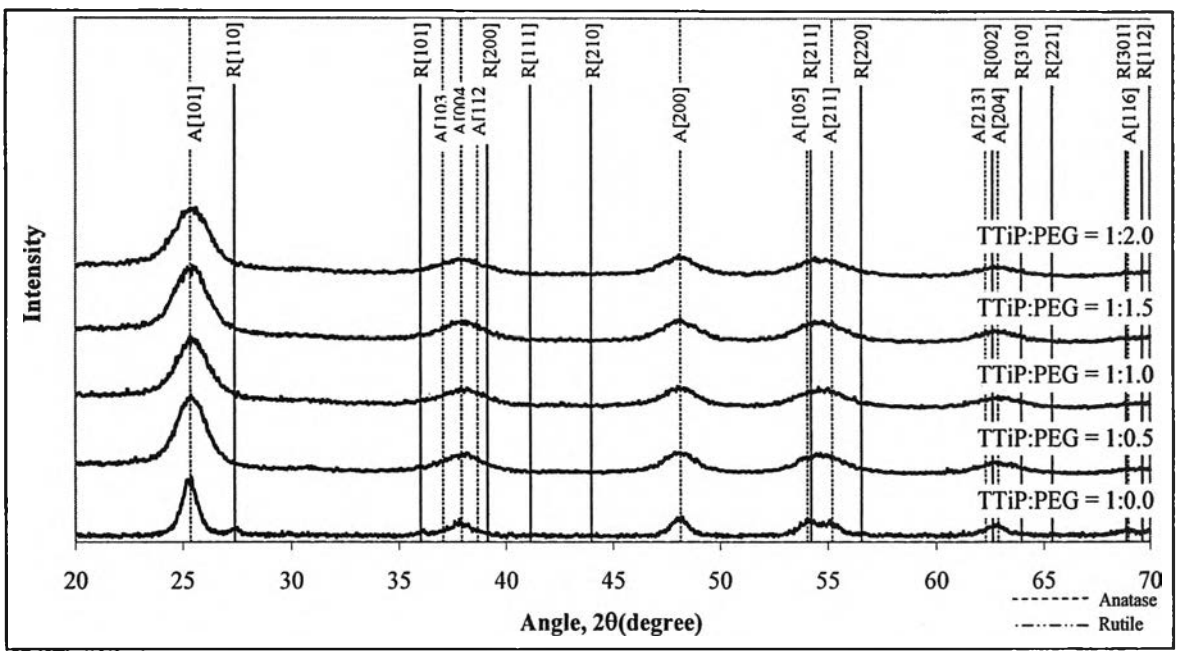

Figure 4.19 XRD spectrum showing Crystal structures of TiO_2 obtained from different mole ratio of TTiP:PEG

As shown in the X-ray diffraction patterns of TiO_2 nanoparticles in Figure 4.19, anatase phase was the predominant structure in all synthesis conditions. A major peak corresponding to (1 0 1) reflections of the anatase phase of TiO_2 is shown at the angle at 25.36°, while the minor peaks are appeared at 48.15° and 54.05°. Peaks for rutile morphology could be found at the angle at 27.39°. It was also found the intensity of anatase peaks was not significantly different as the molar ratio of PEG increased.

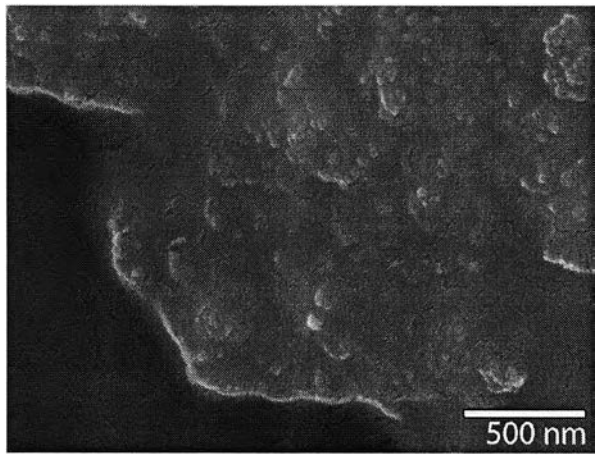

(a) TiO_2 without PEG

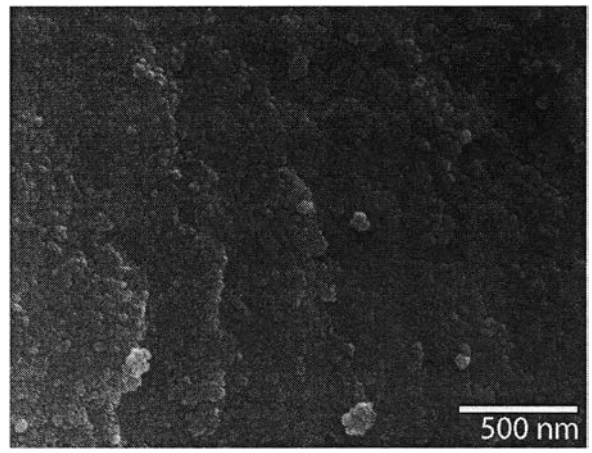

(b) TiO_2 with PEG, TTiP:PEG is 1:0.5

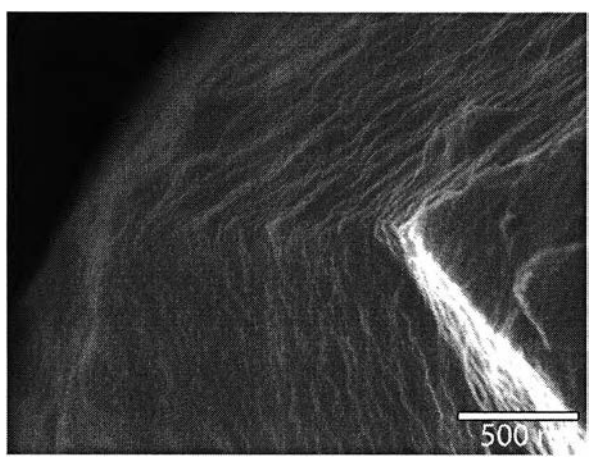

(c) TiO_2 with PEG, TTiP:PEG is 1:1.0

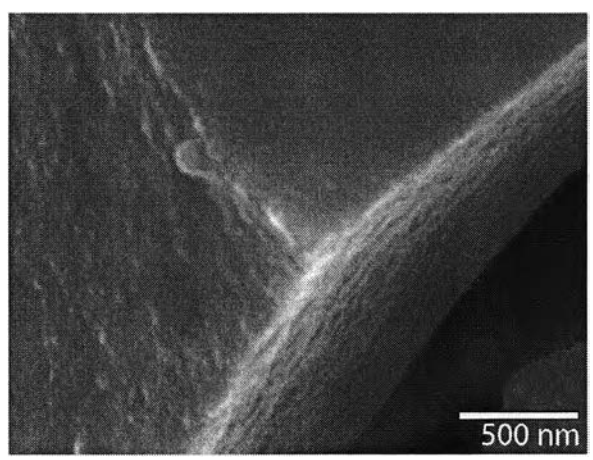

(d) TiO_2 with PEG, TTiP:PEG is 1:1.5

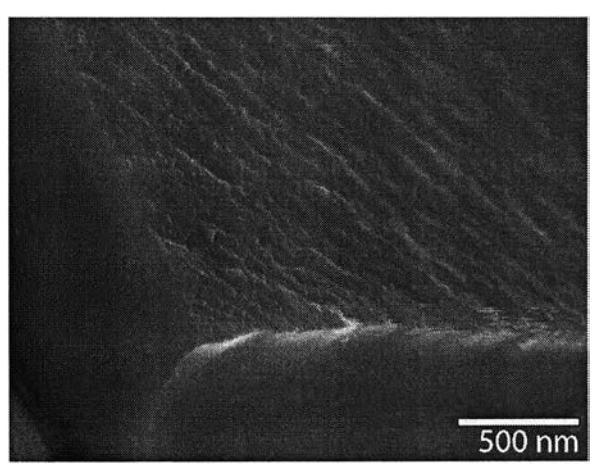

(e) TiO_2 with PEG, TTiP:PEG is 1:2.0

Figure 4.20 SEM images showing surface morphology of TiO_2 nanocrystals obtained from different mole ratios of TTiP:PEG

Recalling that in previous section for the formation of nanocrystal TiO_2 with DEG, it was found that DEG delays the phase transformation of anatase to rutile phase with mole ratio of TTiP:DEG higher than 1:0.5. With the same consideration, it is found that with addition of PEG, the rutile phase was disappeared. This behavior is clearly illustrated by the percentage values of anatase to rutile in each condition as calculated and shown in Table 4.12.

Table 4.12 Percentage of anatase and rutile phases in samples obtained with different mole ratios of TTiP:PEG

Mole ratio of TTiP:PEG	Anatase (%)	Rutile (%)
1:0.0	72.24	27.76
1:0.5	100.00	0.00
1:1.0	100.00	0.00
1:1.5	100.00	0.00
1:2.0	100.00	0.00

The percentage of anatase:rutile of TiO_2 without PEG was calculated as equal to 72.24:27.76. With PEG addition, the rutile phase was not formed at all. From this work, it is clear that PEG halts the progressive of phase transformation from anatase to rutile phase.

Morphologies of TiO_2 with different mole ratios of TTiP:PEG are shown in Figure 4.20. From pictures of TiO_2 nanocrystals, it is obviously that PEG also exerts pronounce effect on reducing of nanocrystal size. As the amount of PEG increase, the TiO_2 nanocrystal size tends to decrease. Apparently, comparing with the TiO_2 morphology in Figure 4.21 (a), the size of TiO_2 with PEG has relatively smaller than that of TiO_2 without any stabilizing agents.

The crystal size of TiO_2 nanopowder as a function of mole ratio of TTiP:PEG is illustrated at Figure 4.21. In this work, it is found that as the amount of PEG increased, the size of TiO_2 crystallites slightly decreased. The crystallite size of anatase phase was decreased from 21.10 nm without any PEG to be 7.91 nm with the 1:2.0 TTiP:PEG. The results suggest that adding PEG the crystallite size of TiO_2 nanoparticles as the same way as DEG does. As a consequence, PEG is expected to

have significant influence on photocatalytic activity due to the increased active surface area of the smaller size of nanoparticles.

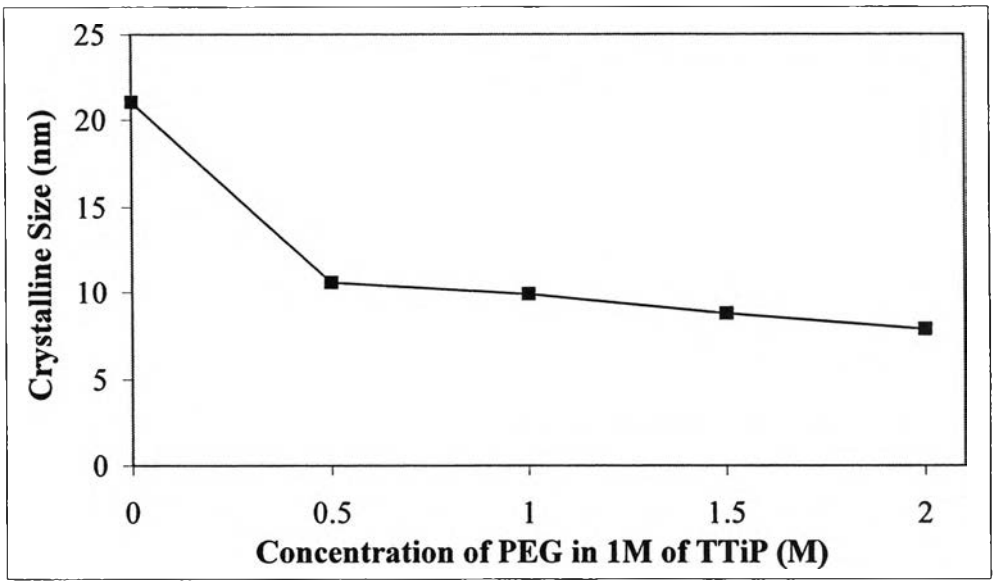

Figure 4.21 Nanocrystal size of TiO_2 with different mole ratios of PEG

The BET surface area of the synthesized TiO_2 was also determined and the results are shown in Figure 4.22. As discussed previously that PEG tends to decrease the crystalline size of TiO_2, this effect is confirmed by the measurement of surface area. If the crystalline size of TiO_2 decreases, the surface area of TiO_2 will be increase simultaneously. The effect of PEG on enhancing the surface area is clearly seen in Figure 4.22. Without any stabilizing agents, the surface area of crystalline size was 83.73 m^2/g. With the PEG addition to the preparation method with the 1:0.5 TTiP:PEG, the surface area of TiO_2 became 208.44 m^2/g. Moreover, surface area of TiO_2 was gradually increased with the increasing of amount of PEG in the sol solution. Finally, the highest surface area of 263.58 m^2/g was obtained with the 1:2.0 TTiP:PEG.

In terms of porosity of the sample set, the pore volumes and the diameter of pores are shown in Table 4.13. In comparison of pore volume and pore size between TiO_2 with PEG and TiO_2 without PEG, the pore volume was increased with the addition of PEG as the pore volume was 0.127 cm^3/g for TiO_2 without PEG and this value was changed to 0.121-0.132 cm^3/g for TiO_2 with PEG. In parallel, the diameter of pore size was 5.98 nm for TiO_2 without PEG and this value was decreased in the range of 3.10-3.35 nm for TiO_2 with PEG. It is worth to note that the differences in

pore volume and pore size with different mole ratios of TTiP:PEG were not obvious in this work.

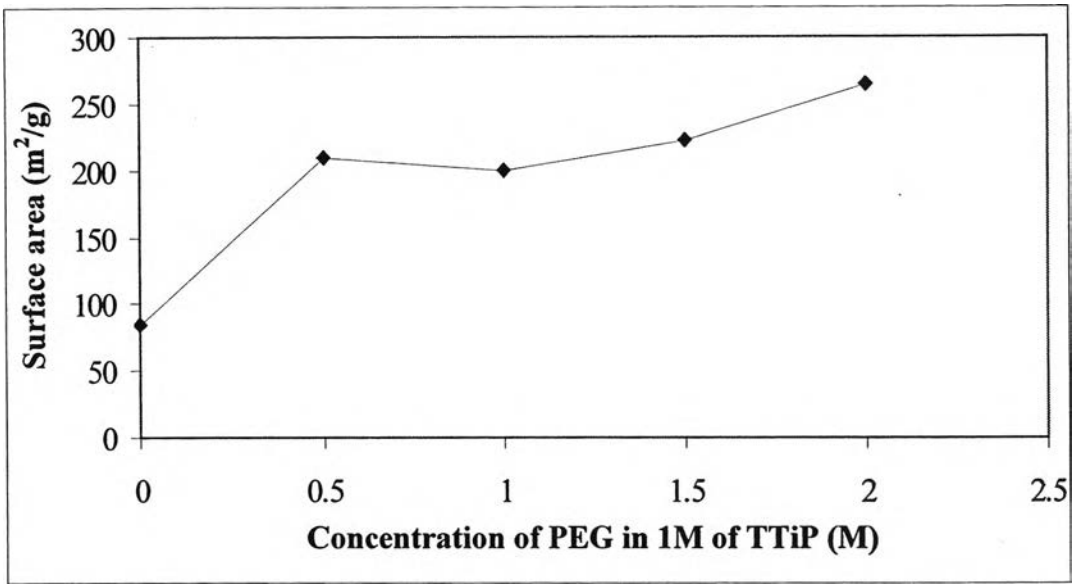

Figure 4.22 Surface area of the synthesized TiO_2 with different mole ratios of PEG

Table 4.13 Porosity of the synthesized TiO_2 with different mole ratios of PEG

Mole ratio of TTiP:PEG	Pore volume (cm^3/g)	Diameter of pore size (nm)
1:0	0.127	5.981
1:0.5	0.184	3.201
1:1.0	0.131	3.103
1:1.5	0.132	3.353
1:2.0	0.121	3.141

4.2.1.2 Photocatalytic activity of nanocrystal TiO_2 with different amounts of PEG

Effects of different amounts of PEG on photocatalytic activity of nanocrystal TiO_2 were studied. In this experimental set, TiO_2 nanoparticles prepared from different mole ratios of TTiP:PEG in the range of 1:0 - 1:2.0 were used and the amount of TiO_2 in each study was fixed at 3 g/L. The experiments in this section were divided into two parts, adsorption and irradiation processes.

In adsorption process, the highest concentrations of adsorbed chromium (VI) on different types of TiO_2 surface were determined. Results of this experimental part are shown in Figure 4.23. It was found that the contact time to reach the equilibrium was 60 minutes. Apparently, the equilibrium concentrations of chromium (VI) in the aqueous solution using different types of TiO_2 were not significantly different. The adsorbed chromium (VI) was in the range of 0.692 - 1.182 mg Cr(VI)/g TiO_2. Adsorption data reveal that the 4.15 - 7.10% of the total amount of chromium (VI) in the reactor was adsorbed on the catalyst surface.

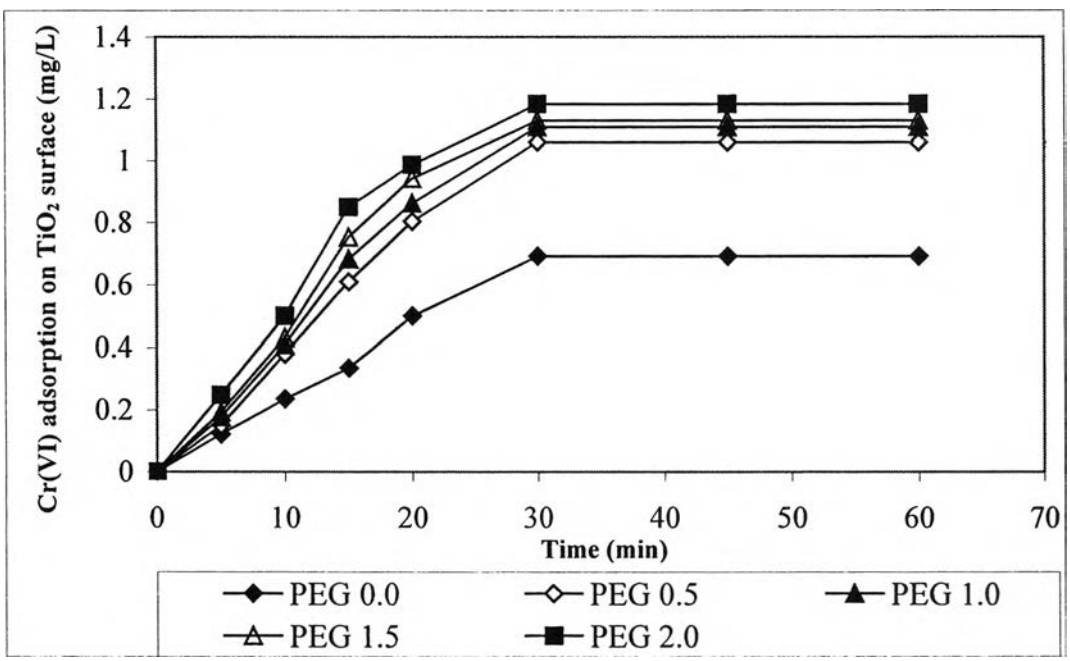

Figure 4.23 Adsorption of Cr (VI) on the surface of TiO_2 prepared with different mole ratios of TTiP:PEG

The photocatalytic reduction of chromium (VI) under irradiation process for the nanocrystal TiO_2 with different mole ratios of TTiP:PEG was compared. The ratio of residual to initial concentration of chromium (VI) in term of C/C_0 as a function of irradiation time was illustrated in Figure 4.24. It is obvious that the nanocrystal TiO_2 prepared with PEG provided the higher efficiency in chromium (VI) removal comparing to the TiO_2 without PEG. In consideration of treating efficiency of chromium (VI) using different mole ratio of TTiP:PEG, it was found that there is not much difference in chromium (VI) removal from each condition as presented in the previous section, the nanoparticle size, pore volume, and pore size were not much different when TTiP:PEG was in the range of 1:1.0 –1:2.0. Therefore, the

photocatalytic activities obtained from these three conditions were not significantly different.

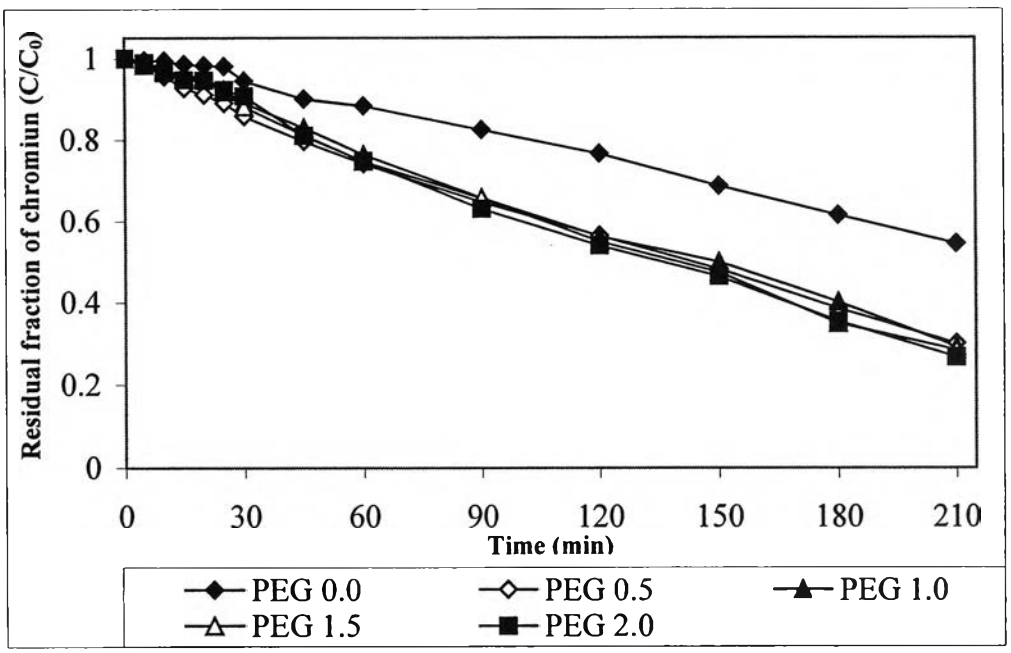

Figure 4.24 Photocatalytic reduction of chromium (VI) using different mole ratios of TTiP:PEG

The plot of k_{obs} as a function of the amount of PEG presented in titania from each condition is shown in Figure 4.25. This figure shows that k_{obs} obtained from TiO_2 with mole ration of TTiP:PEG as 1:2.0 was slightly higher than other conditions (Table 4.14). This behavior can be explained in terms of the surface area. The photocatalytic reaction is confined mostly to the surface of the TiO_2 nanoparticles under illumination. Therefore, the higher the surface area, the more the photocatalytic reaction occurs (Yoon et al., 2006) and the mole ratio of 1:2.0 TTiP:PEG provided the smallest size of nanocrystal TiO_2, highest surface area and porosity, the highest photocatalytic activity could be found at this condition.

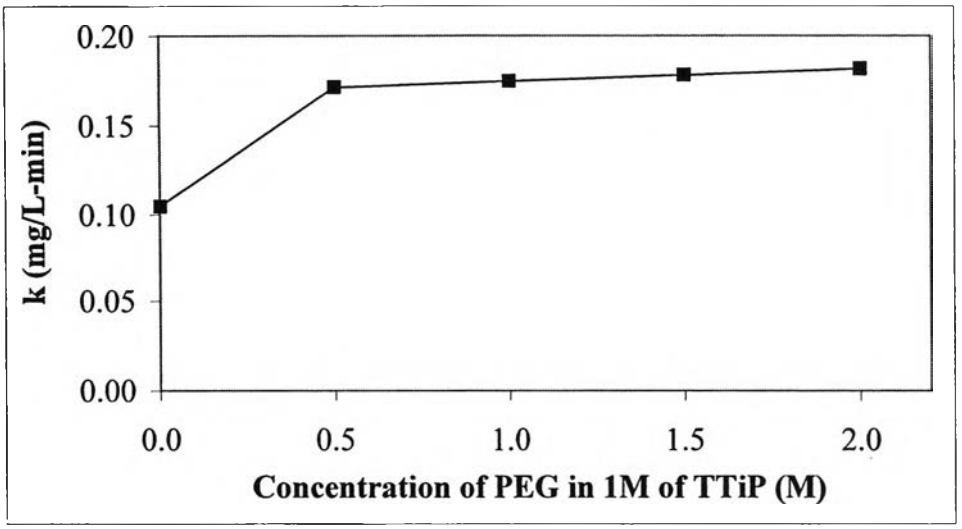

Figure 4.25 Comparison of photocatalytic decomposition rates using different mole ratios of TTiP:PEG

Table 4.14 Value of k_{obs} and chromium removal efficiencies of TiO_2 prepared from different mole ratios of TTiP:PEG

Mole ratio of TTiP:PEG	k_{obs} (mg/L-min)	R^2	% Removal
1: 0.0	0.1041	0.9898	47.67
1: 0.5	0.1712	0.9939	71.89
1: 1.0	0.1754	0.9850	73.29
1:1.5	0.1785	0.9934	73.88
1: 2.0	0.1813	0.9926	75.40

4.2.2 Crystal growth of TiO_2 with PEG

4.2.2.1 Effect of calcination temperatures on nanocrystal TiO_2 with PEG

To study the effect of calcination temperature on nanocrystal TiO_2, the mole ratio of TTiP:PEG was fixed at 1:1.0 and the calcination temperatures were varied as 300, 450, 500, 600, and 800 °C. The crystal structures of TiO_2 from each condition obtaining from X-ray diffraction analysis are illustrated in Figure 4.26.

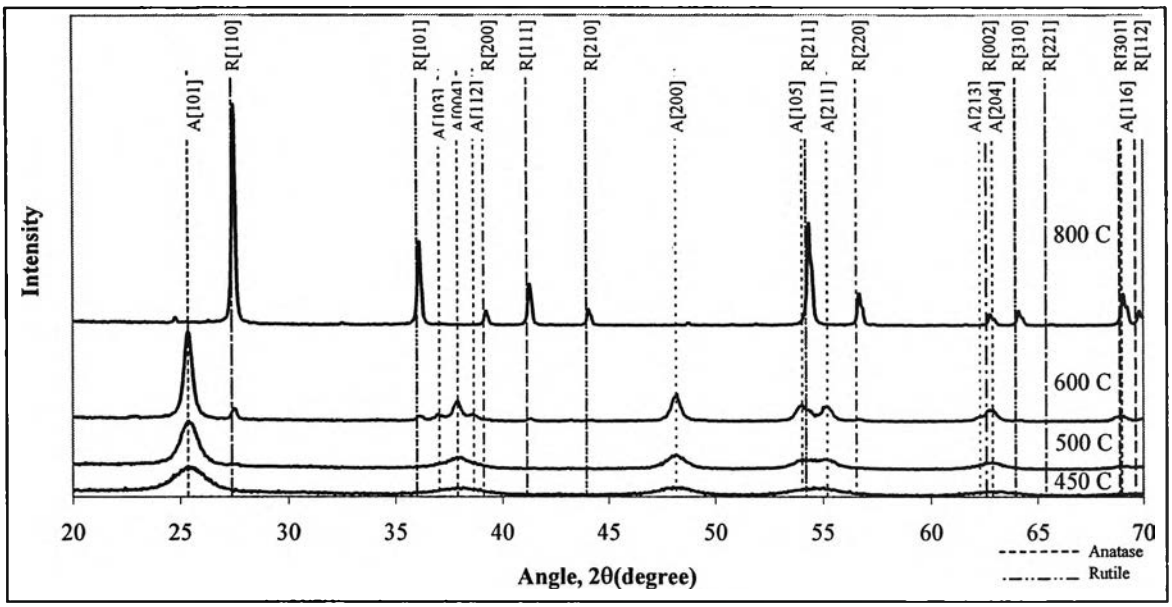

Figure 4.26 Crystal structures of TiO_2 with PEG stabilizing agents in different calcination temperatures

As shown in Figure 4.26, anatase phase with a major peak corresponding to (1 0 1) was the predominant structure for the TiO_2 calcined at 300-600 °C. The growth of anatase was increased with the higher calcination temperature as shown in the figure. Rutile phase with a major peak corresponding to (1 1 0) was developed with the 600 °C calcination temperature while the intensity corresponding to the anatase phase was reduced sharply. It is worth to note that the transformation of anatase to rutile phase of TiO_2 without PEG was developed at 450 °C and the transformation phase was developed at 800 °C with PEG addition. Percentages of anatase and rutile phases were also calculated to compare the phase transformation of TiO_2 between TiO_2 synthesis with PEG stabilizing agents and without PEG as shown in Table 4.15.

Table 4.15 Percentages of anatase and rutile phases in samples obtained from different calcination temperatures

Calcination temperature (°C)	TiO_2 without stabilizing agents		TiO_2 with PEG	
	Anatase (%)	Rutile (%)	Anatase (%)	Rutile (%)
300 °C	100.00	0.00	100.00	0.00
450 °C	72.24	27.76	100.00	0.00
500 °C	42.02	57.98	100.00	0.00
600 °C	11.59	88.41	86.52	13.48
800 °C	0.00	100.00	0.00	100.00

From this experimental set, rutile phase in TiO_2 without any stabilizing agents was formed in lower calcination temperature than the TiO_2 with PEG. At the 500 °C calcination temperature almost 60% of anatase phase in the TiO_2 without PEG has been transformed into rutile but no rutile phase was formed in the TiO_2 with PEG. With the same trend, at the 600 °C calcination temperature percentage ratio of anatase to rutile was 11.59:88.41 in the TiO_2 without PEG, while this ratio was changed to 86.52:13.48 with the addition of PEG. At 800 °C, anatase was disappeared for both TiO_2 without PEG and TiO_2 with PEG.

Apparently, results from this work indicate that PEG also delays the transformation of anatase to rutile phase at a high temperature, which is the same effect with DEG but the deferral is shown in different calcination temperature.

The surface morphologies of TiO_2 nanocrystals from each condition are shown in Figures 4.27 (a)-(e). It is obvious that the surface morphological was different with the variation of different calcination temperatures in the range of 300-600 °C. The effect of the calcination time upon the grain size of TiO_2 powders is clearly shown in this figure. As calcination temperature was lower than 450 °C, the prolongation of calcination time has little influence upon the particle size. However when the calcination temperature was leveled up, the obvious influence upon grain size was found. The size of nanocrystal TiO_2 obtained at 800°C calcination temperature was the biggest size comparing to those obtained from the lower calcination temperatures.

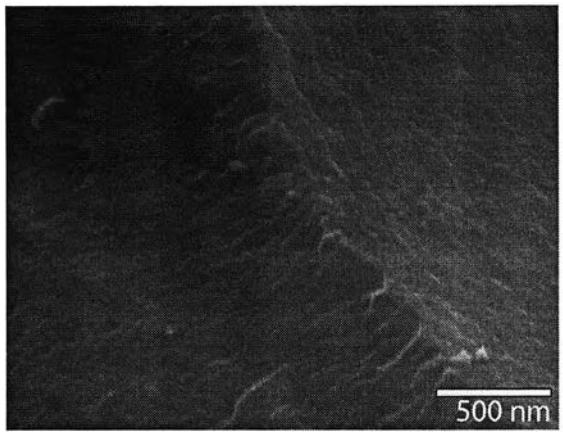

(a) TiO_2 calcined at 300 °C

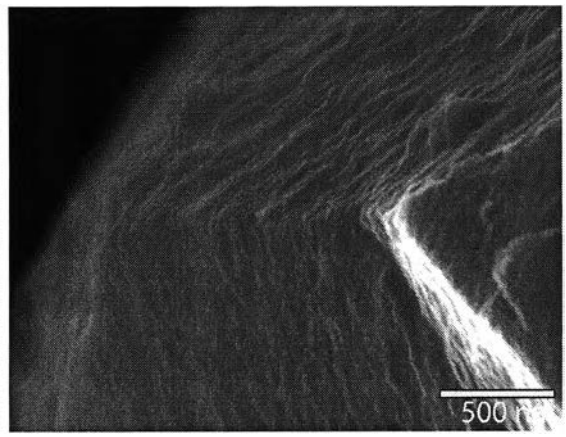

(b) TiO_2 calcined at 450 °C

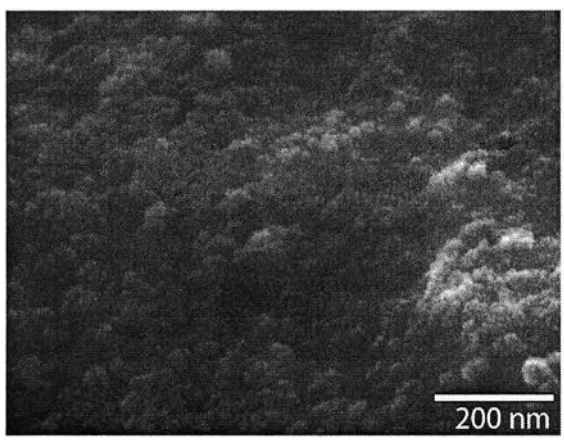

(c) TiO_2 calcined at 500 °C

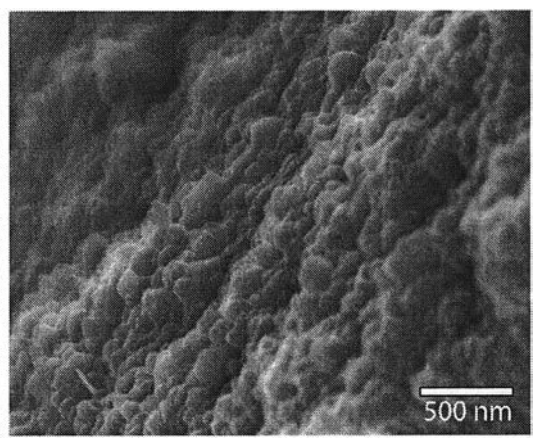

(d) TiO_2 calcined at 600 °C

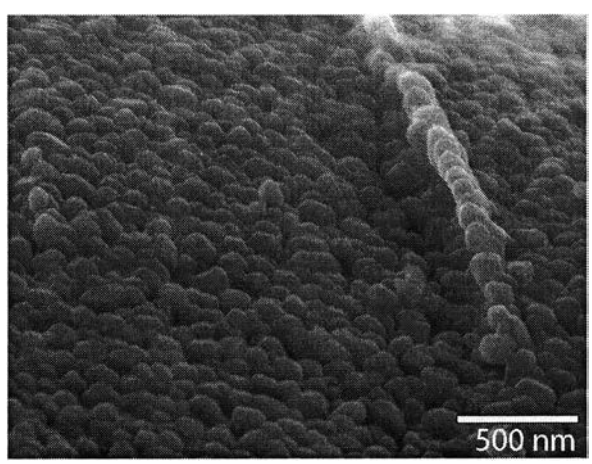

(e) TiO_2 calcined at 800°C

Figure 4.27 SEM images showing surface morphology of TiO_2 nanocrystal with PEG in different calcination temperatures

To determine that growth of nanocrystal TiO_2 was dependent on the calcination temperature, the sizes of nanocrystal TiO_2 from each condition were calculated using Debye-Scherrer equation. Summary of size variation of TiO_2 nanocrystal synthesized with PEG stabilizing agent and the calcination temperatures

is shown in Table 4.16. The size variation of TiO_2 nanocrystal synthesized without any stabilizing agents is also included in the same table for comparison.

Table 4.16 Size of anatase and rutile TiO_2 in samples prepared at different calcination temperatures

Calcination temperature (°C)	TiO_2 without PEG		TiO_2 with PEG	
	Anatase (nm)	Rutile (nm)	Anatase (nm)	Rutile (nm)
300	9.31	-	-	-
450	21.10	37.45	9.89	-
500	31.03	56.18	18.40	-
600	39.57	76.24	32.97	73.61
800	-	76.24	-	142.32

Considering the effect of PEG on particle growth of TiO_2, it was found that, in average, size of nanocrystal TiO_2 with PEG stabilizing agent was smaller than those without PEG. Normally, the particle size of anatase is smaller than the rutile. As discussed previously, at the calcination temperature lower than 600 °C, the phase of TiO_2 with PEG was fully anatase, while phase of TiO_2 without PEG contained both anatase and rutile. The difference in phase of TiO_2 is expected to be the result of the difference in nanosize of TiO_2.

At the calcination temperature of 300 °C, TiO_2 was in amorphous form, thus, the nanosize cannot be defined. As the calcination temperature increased to 450 °C, the nanosizes of TiO_2 with PEG in anatase form were determined as 9.89 nm. This value was increased to 18.40 nm with higher calcination temperature at 500 °C. Above 600 °C, growth of TiO_2 was clearly observed due to the transformation of anatase to rutile phase. For rutile, the crystal size was increased drastically from 73.61 nm at 600°C to 142.32 nm at 800°C. For anatase, the nanocrystal size of titania was reduced from 32.97 nm at 600 °C calcination temperature to 9.89 nm at 450 °C.

Table 4.17 shows the surface area of TiO_2 prepared from the range of above calcination temperatures. It can be clearly seen that, when comparing the surface areas of TiO_2 without PEG and TiO_2 with PEG, PEG not only decreases the size of nanoparticles but also increases the surface area of nanoparticles. When varying calcination temperature, the surface area of TiO_2 was drastically changed. As

calcination temperature increased, the size of nanoparticle increases resulting in the reduced surface area. Moreover, the calcination temperature leads to the phase transformation from anatase to rutile yielding the increasing of pore diameter with the exception when TiO_2 is in the amorphous phase, which is formed at 300 °C calcination temperature.

Table 4.17 Surface area and pore diameter of TiO_2 prepared with and without PEG at different calcination temperatures

Calcination temperature (°C)	TiO_2 without PEG		TiO_2 with PEG	
	Surface area (m^2/g)	Pore diameter (nm)	Surface area (m^2/g)	Pore diameter (nm)
300 °C	174.50	2.285	1.58	1.501
450 °C	83.73	5.981	199.40	3.103
500 °C	22.20	5.914	109.60	4.969
600 °C	0.52	17.830	30.97	9.797
800 °C	0.43	12.670	1.17	31.670

4.2.2.2 Photocatalytic activity of nanocrystal TiO_2 prepared with DEG at different calcination temperatures

Effects of calcination temperature on photocatalytic activity of nanocrystal TiO_2 were studied. In this experimental set, TiO_2 nanopowders obtained previously at calcination temperatures in the range of 300 °C to 600 °C were used and the amount of TiO_2 in each study was fixed at 3 g/L. The experiments in this section were divided into two parts, adsorption and irradiation process.

In adsorption process, the highest concentrations of adsorbed chromium (VI) on TiO_2 surface using different types of TiO_2 were determined. Results of this experimental part are shown in Figure 4.28. It was found that the contact time to reach the equilibrium was 60 minutes. The equilibrium concentrations of chromium (VI) in the aqueous solution using different types of TiO_2 were considerably different. The adsorbed chromium (VI) was in the range of 0.309-0.995 mg Cr (VI)/g TiO_2. Adsorption data revealed that the 1.86-5.97% of the total amount of chromium (VI) in the reactor was adsorbed on the catalyst surface. Generally, the major factor affecting the adsorption process is surface area of TiO_2. Thus, since the TiO_2 from 450 °C

calcination temperature provided the smallest size of 4.14 nm and the highest surface area of 199.40 m^2/g, the TiO_2 from this condition can attract the highest amount of chromium (VI) on the particle surface.

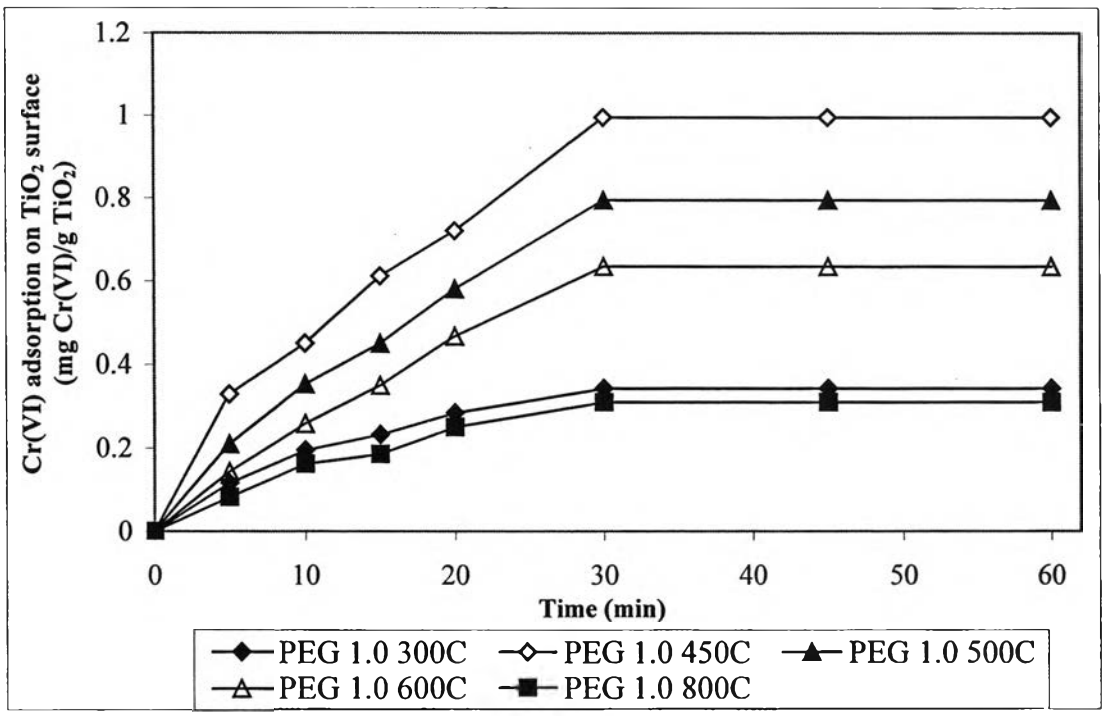

Figure 4.28 Adsorption of chromium (VI) on the surface of TiO_2 prepared At different calcination temperatures as a function of time

The photocatalytic reduction of chromium (VI) under irradiation process for the nanocrystal TiO_2 with different calcination temperatures was compared. The ratio of residual to initial concentration of chromium (VI) in term of C/C_0 as a function of irradiation time was illustrated in Figure 4.29. It obvious that the nanocrystal TiO_2 prepared at 500 °C calcination temperature provided the highest efficiency in chromium (VI) removal compared to other conditions. It is worth to note that the TiO_2 prepared at 450°C calcination temperature provided the highest amount of chromium (VI) adsorption on titania surface, while the TiO_2 prepared at 500°C calcination temperature provided the highest amount of chromium (VI) reduction upon irradiation process. This may be due to the fact that beyond 600 °C there was the transformation of anatase to rutile phase. Moreover, the growth of TiO_2 crystal was clearly seen as the crystal in rutile phase was bigger than the crystal of anatase phase yielding the decreasing in surface area of the titania. With both factors (crystal phase and surface

area), the decreasing of photocatalytic reduction of chromium (VI) was seen in this experiment.

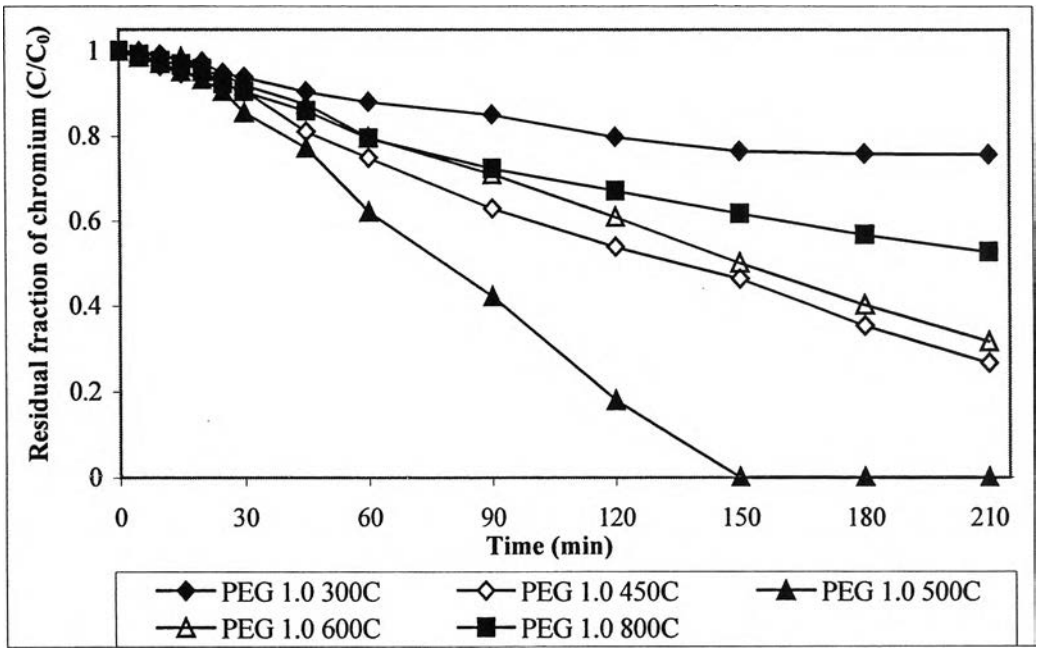

Figure 4.29 Photocatalytic reduction of chromium (VI) by TiO_2 prepared at different calcination temperatures as a function of time

In term of kinetics, the photocatalytic reduction reactions of chromium (VI) of nanocrystal TiO_2 obtained from various calcination temperatures were followed the zero-order pattern. The values of k_{obs} were calculated and the plots of k_{obs} as a function of calcination temperature are shown in Figure 4.30. This figure shows that k_{obs} increased with increasing calcination temperatures. However after reached the highest value for sample of 500 °C calcination temperature, the value of k_{obs} decreased. From this information, the photocatalytic activity as represented by the k_{obs} is mainly governed by the anatase phase of TiO_2. At calcination temperature higher than 500 °C, crystal phase was transformed to rutile, causing the decreased of photocatalytic activity. Moreover, in PEG addition, the crystal size of TiO_2 was strongly depended on the calcination temperature, as the rutile is formed, the crystal growth is clearly observed and the surface area of TiO_2 crystal is drastically decreased. The decreasing in surface area of TiO_2 is another reason that might effect in the decreasing of the photocatalytic activity as well in this case. Thus, in overall consideration, the TiO_2 with 500 °C calcination temperature provided the best condition for chromium (VI) removal.

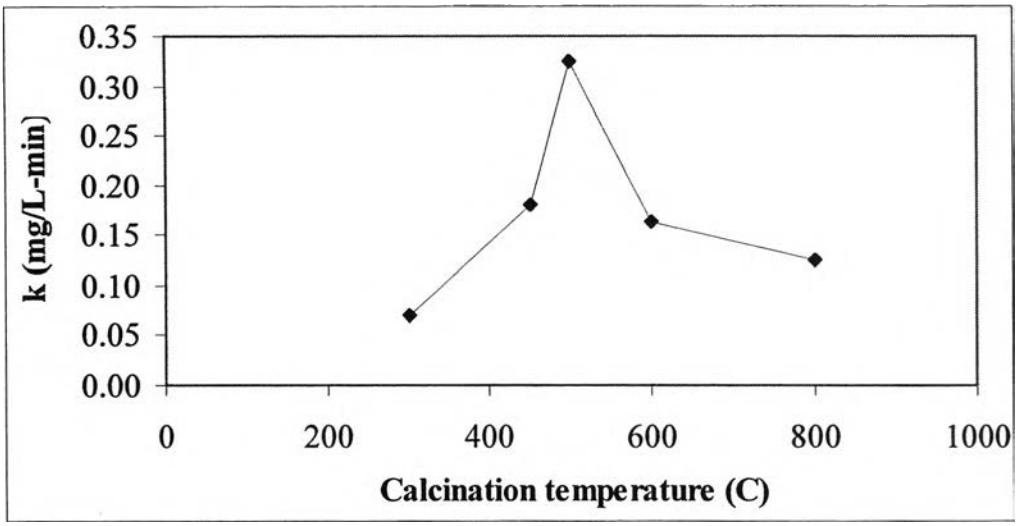

Figure 4.30 Comparison of photocatalytic decomposition rates using different calcination temperatures

4.2.3 Determination of adsorption isotherm of TiO_2 with PEG as additive

To obtain the adsorption characteristic of TiO_2 with PEG, it is necessary to determine the adsorption isotherm of the titania. The best condition learned from the previous section (TTiP:PEG mole ratio = 1:1, and 500 °C calcination temperature) was used in this part. The adsorption of chromium (VI) with TiO_2 as the initial concentration of chromium (VI) varied in the range of 10-100 mg/L was conducted. The results of this experimental part are shown in Figure 4.31. It is obvious that the amount of chromium (VI) adsorbed on titania surface is increased with increasing initial concentration of chromium (VI) in the water.

To obtain the adsorption isotherm of TiO_2, the plot of adsorbed chromium (VI) on titania surface (mg Cr(VI)/mg TiO_2) versus the concentration of chromium (VI) in the solution after reaching the equilibrium (mg/L) was performed as shown in Figure 4.32. The value of adsorbed chromium (VI) on titania surface was increased with increasing of the equilibrium concentration of chromium (VI) until it reached the certain value and the plateau of the adsorption pattern was obtained.

The values of chromium (VI) adsorption at equilibrium condition were used further in determining adsorption isotherm in both Langmuir and Freundlich equations.

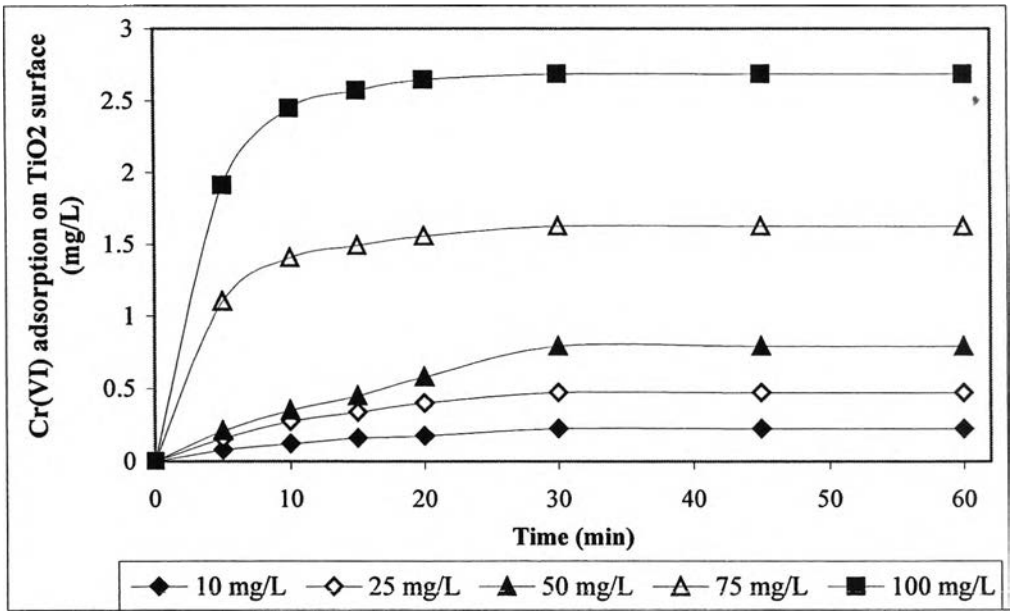

Figure 4.31 Adsorption of chromium (VI) on the surface of TiO_2 at different initial concentration of chromium (VI) as a function of time

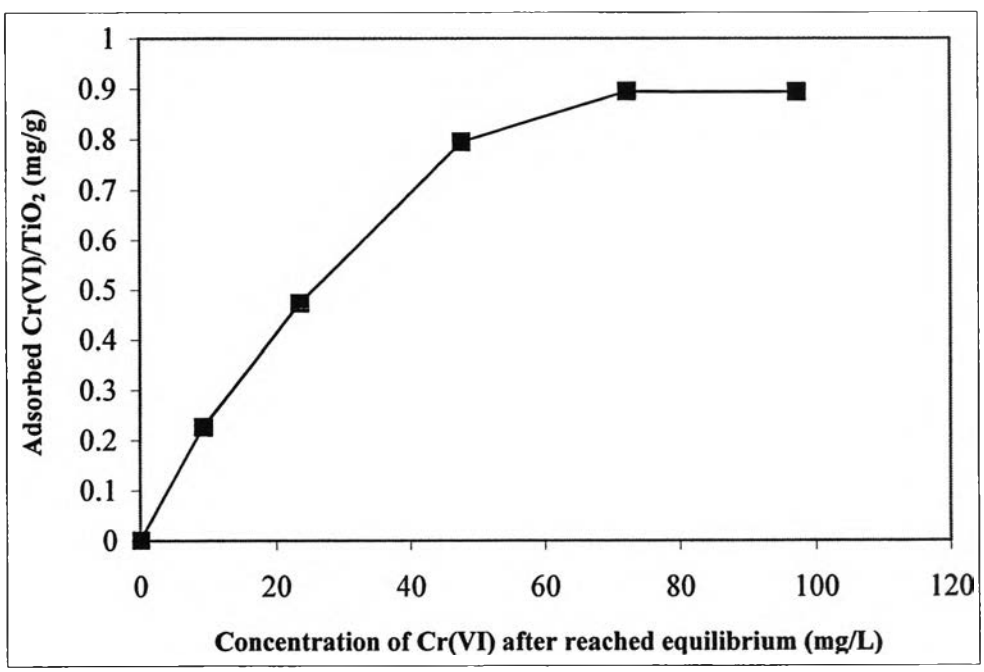

Figure 4.32 Plot of chomium (VI) equilibrium concentration vs. chromium (VI) adsorbed concentration on TiO_2 surface

The Langmuir equation was applied for the adsorption equilibrium of chromium (VI) onto TiO_2 surfaces. The Langmuir equation is shown below:

$$\frac{C_e}{(x/m)} = \frac{1}{(Q_0 b)} + \frac{C_e}{Q_0} \qquad (4.28)$$

where C_e is the equilibrium concentration of chromium (VI), mg/L, *(x/m)* is the amount of adsorbed chromium (VI) at equilibrium per unit mass of TiO_2, mg/g, and Q_0 and b are Langmuir constants related to adsorptive capacity and energy of adsorption, respectively.

The linear plot of $C_e/(x/m)$ vs. C_e in Figure 4.33 shows that the adsorption of chromium (VI) onto the TiO_2 surface obeys the Langmuir adsorption isotherm. The correlation coefficient for the linear regression fit of the Langmuir plot was found to be 0.9654. The expressed equation is

$$\frac{C_e}{(x/m)} = 0.7477 C_e + 30.749 \qquad (4.29)$$

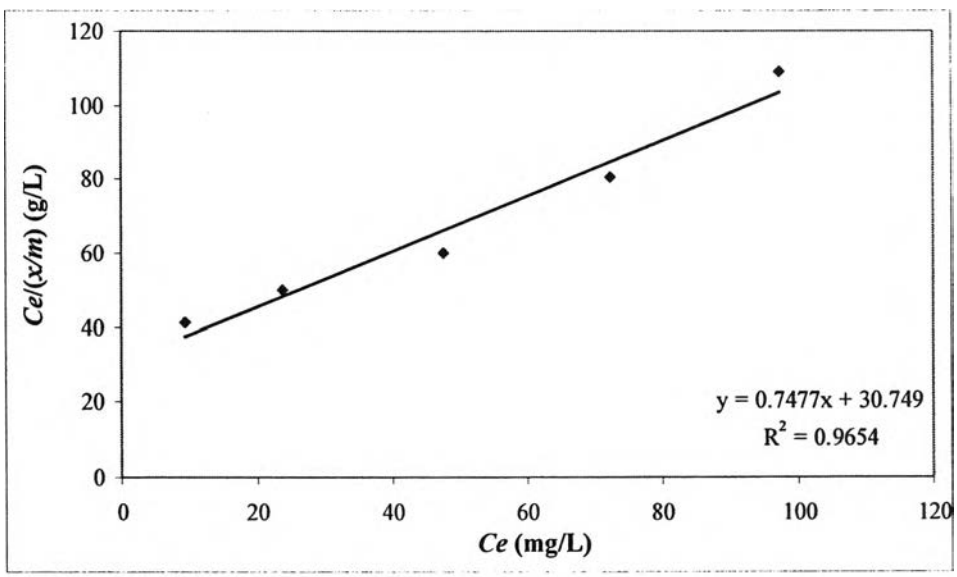

Figure 4.33 Langmuir adsorption isotherm plots
for the adsorption of chromium (VI) onto the TiO_2 surface

The Langmuir constants Q_0 and b were determined from the Langmuir plots and found to be 1.34 mg/g and 0.024 L/mg respectively. The essential characteristic of the Langmuir isotherm can be expressed in terms of a dimensionless constant separation factor or equilibrium parameter, R_L. The values of R_L in this experiment set

were calculated as shown in Table 4.18 and it was found that all values are between 0 and 1, indicating favorable chromium (VI) adsorption onto the TiO_2 surface.

Table 4.18 Value of R_L for Langmuir adsorption isotherm for TiO_2 with PEG

Initial concentration of chromium (VI) (mg/L)	**R_L Value**
10	0.85
25	0.69
50	0.52
75	0.42
100	0.36

The Freundlich equation was also applied to describe the adsorption of chromium (VI) onto the TiO_2 surface. The Freundlich equation is basically empirical, and generally agrees with the experimental data over a moderate range of adsorbate concentrations. The Freundlich isotherm is represented by the equation (Mckay et al., 1982)

$$\log(x/m) = (1/n)\log C_e + \log k_f \qquad (4.30)$$

where C_e is the equilibrium concentration of chromium (VI), mg/L, (x/m) is the amount of adsorbed chromium (VI) at equilibrium per unit mass of TiO_2, mg/g, and k_f and n are the Freundlich constants.

The linear plot of log (x/m) vs. log C_e in Figure 4.34 shows that the adsorption of chromium (VI) onto the TiO_2 surface obeys the Freundlich adsorption isotherm.

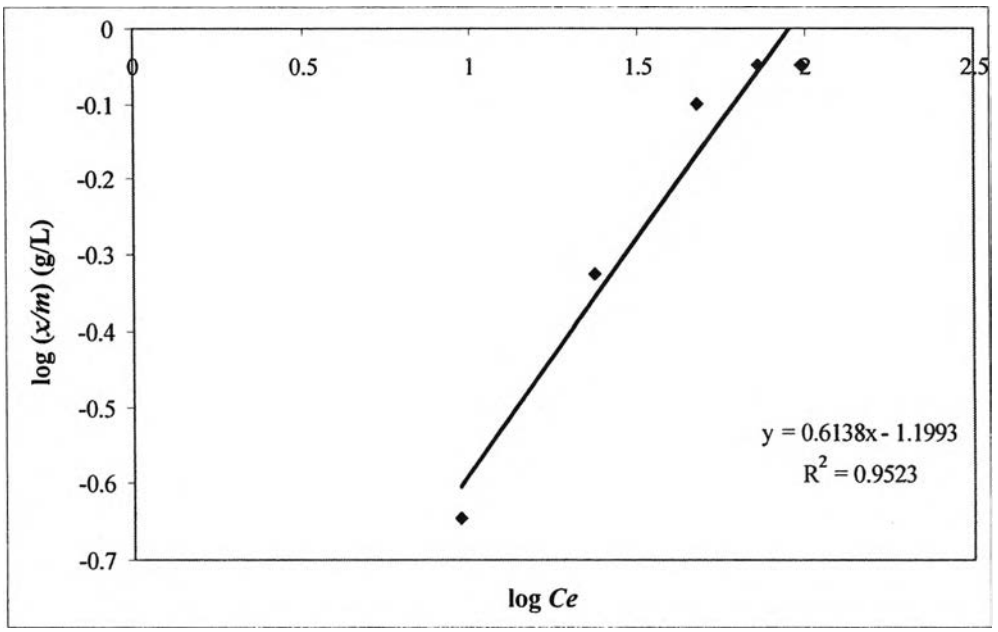

Figure 4.34 Freundlich adsorption isotherm plots
for the adsorption of chromium (VI) onto TiO_2 surface

The expressed equation is

$$\log(x/m) = 0.6138 \log C_e - 1.1993 \qquad (4.31)$$

The correlation coefficient for the Freundlich plot was found to be 0.9523, which was less than that from the Langmuir plot. The value of correlation coefficient of chromium (VI) adsorption indicates that the adsorption behavior of chromium (VI) onto TiO_2 tends to be a monolayer adsorption as described by the Langmuir isotherm rather than the Freundlich isotherm.

4.2.4 Determination of kinetic values following Langmuir-Hinshelwood Model for TiO_2 with PEG stabilizing agent

Additional kinetic values were obtained using Langmuir-Hinshelwood model. The best condition from the previous section (TTiP:PEG mole ratio = 1:1, and 500°C calcination temperature) is used in this part. The photocatalytic reduction of chromium (VI) by TiO_2 with variation of initial concentration of chromium (VI) in the range of 10-100 mg/L was conducted.

The results of this experimental part are shown in Figure 4.35. It is obvious that the amount of chromium (VI) adsorbed on titania surface is increased with the increasing of initial concentration of chromium (VI) in the water. The values of k_{obs} from zero-order and pseudo-first order equations were also determined as shown in Table 4.19 and Table 4.20.

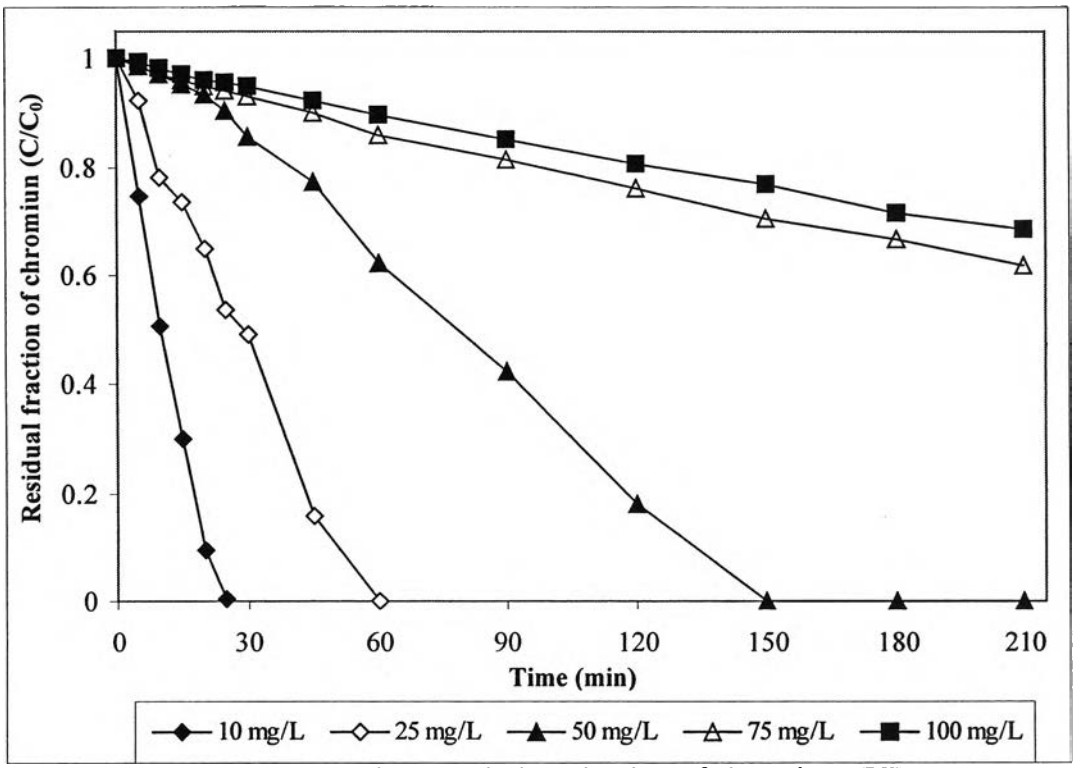

Figure 4.35 Photocatalytic reduction of chromium (VI) using different initial concentration of chromium (VI) as a function of time

Table 4.19 Values of k_{obs} from zero-order equation for photocatalytic process using TiO_2 with PEG for chromium (VI) removal

Initial concentration of chromium (VI) (mg/L)	k_{obs} (mg/L-min)	R^2	% Removal	Final concentration of chromium (VI) (mg/L)
10	0.4347	0.9773	100.00	0.00
25	0.4381	0.9902	100.00	0.00
50	0.3235	0.9830	100.00	0.00
75	0.2018	0.9922	42.32	43.26
100	0.1556	0.9922	35.00	65.00

Table 4.20 Values of k_{obs} from pseudo-first order equation for photocatalytic process using TiO_2 with PEG for chromium (VI) removal

Initial concentration of chromium (VI) (mg/L)	k_{obs} (min^{-1})	R^2	**% Removal**	**Final concentration of chromium (VI) (mg/L)**
10	0.1572	0.7316	100.00	0.00
25	0.0317	0.8570	100.00	0.00
50	0.0080	0.9049	100.00	0.00
75	0.0023	0.9966	42.32	43.26
100	0.0018	0.9993	35.00	65.00

Considering the pattern of kinetic equation, the photocatalytic reduction reactions of chromium (VI) by TiO_2 with PEG can be represented by zero-order pattern when initial concentration was relatively low in the range of 10-50 mg/L. However, as concentration of chromium (VI) was leveled up, the kinetic pattern was changed from the zero-order pattern to the first-order pattern as represented by the R^2 values. The change of the reaction behavior can be explained that at low level of chromium (VI) concentration, the reaction was dependent only on the reaction time and it was independent from the concentration of chromium (VI) in the aqueous solution. The surface of titania was not the limitation of the reaction. As chromium (VI) concentration increased with the fixed dosage of TiO_2 in the system, the reaction became dependent on both concentration of chromium (VI) and the reaction time. Results from this experiment set provide the important information that at low level of contaminant concentration, the reaction can be described by zero-order pattern and at high level of contaminant concentration, the reaction is best described by pseudo first-order pattern.

The value of k_{obs} obtained from the pseudo first order pattern can be used further to find the intrinsic kinetic coefficient occurred during irradiation process of photocatalysis. The intrinsic kinetic values of photocatalysis can be determined from the Langmuir-Hinshelwood model.

To obtain a kinetic value for both k_c and K_{cr}, the experiment with initial chromium (VI) concentration as of 60, 70, 80, and 90 mg/L were added. The values of k_{obs} from pseudo-first order equation were calculated and shown in Table 4.21.

Table 4.21 Values of k_{obs} used in Langmuir-Hinshelwood model for photocatalytic process using TiO_2 with DEG for chromium (VI) removal

Initial concentration of chromium (VI) (mg/L)	k_{obs} (min^{-1})	R^2	**% Removal**	**Final concentration of chromium (VI) (mg/L)**
60	0.0027	0.9955	43.28	34.03
70	0.0024	0.9990	42.45	40.29
75	0.0023	0.9966	42.32	43.26
80	0.0022	0.9970	37.00	50.40
90	0.0020	0.9985	36.52	57.13
100	0.0018	0.9993	35.00	65.00

Figure 4.36 shows that the linear expression also can be obtained by plotting the reciprocal of degradation rate ($1/k_{obs}$) as a function of the initial chromium (VI) concentration. By means of a least square best fitting procedure, the values of the adsorption equilibrium constant (K_{Cr}), and the second-order rate constant (k_c) were obtained, and this value found to be K_{Cr} = 0.480 L/mg and k_c = 0.220 mg/L min (R^2 = 0.9958), respectively.

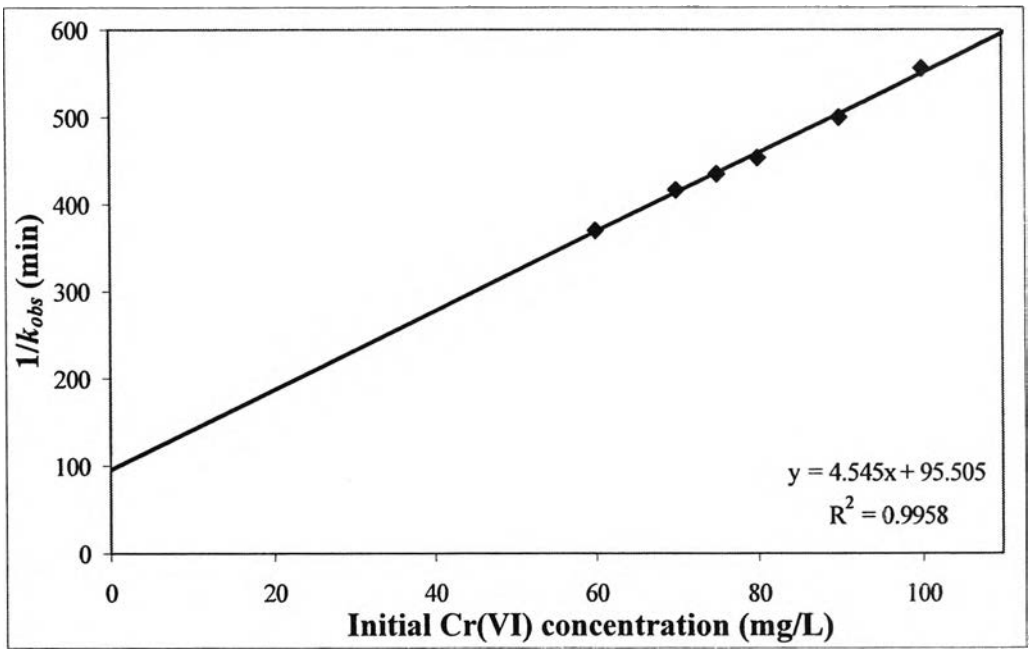

Figure 4.36 Photocatalytic reduction of chromium (VI) using TiO_2 with PEG as a function of initial concentration of chromium (VI)

สำนักงานวิทยทรัพยากร
จุฬาลงกรณ์มหาวิทยาลัย

4.3 Roles of DEG and PEG 600 on TiO_2 Properties and Photocatalytic Activity

4.3.1 Roles of DEG and PEG 600 on the formation of nanocrystal TiO_2

As shown in previous sections, both DEG and PEG 600 exerted key effects on TiO_2 properties and photocatalytic activity. The difference of DEG and PEG 600 is only the short chain and long chain of polyethylene glycol respectively as exhibited in Figure 4.37.

	(a)	(b)
	DEG	**PEG 600**
Formula	$(C_2H_4O)_2 \cdot H_2O$	$(C_2H_4O)_n \cdot H_2O$
M.W.	62.07	600

Figure 4.37 Molecular structures and formula of DEG and PEG 600

Considering roles of DEG and PEG 600 in forming of nanocrystal TiO_2, the XRD patterns for TiO_2 without any stabilizing agents, with DEG and with PEG 600 were compared as depicted in Figure 4.38. Note the phase transformations from anatase to rutile in each set of data. Both DEG and PEG 600 delay the transformation from anatase to rutile phase compared with the XRD patterns of TiO_2 without stabilizing agents. In comparison the effect of short and long chain of polyethylene glycol in DEG and PEG 600, the PEG accelerates the formation of rutile at a lower calcination temperature of 600 °C than the short chain of DEG in which the rutile phase appeared at 800 °C as shown in Figure 4.38. The lower temperature transformation of TiO_2 from anatase to resulted rutile phase by PEG 600 is expected to affect the overall properties of TiO_2 as well.

To discuss the residual of DEG and PEG 600 in the TiO_2 crystal after calcination at high temperature process, the thermo gravimetric analysis (TGA) was performed in the temperature range of 40-800°C with a heating rate of 10°C/min in a dried nitrogen atmosphere to minimize oxidation. The thermo gravimetric analysis of TiO_2 in three conditions: without any stabilizing agents, with DEG and with PEG 600 are shown in Figure 4.39.

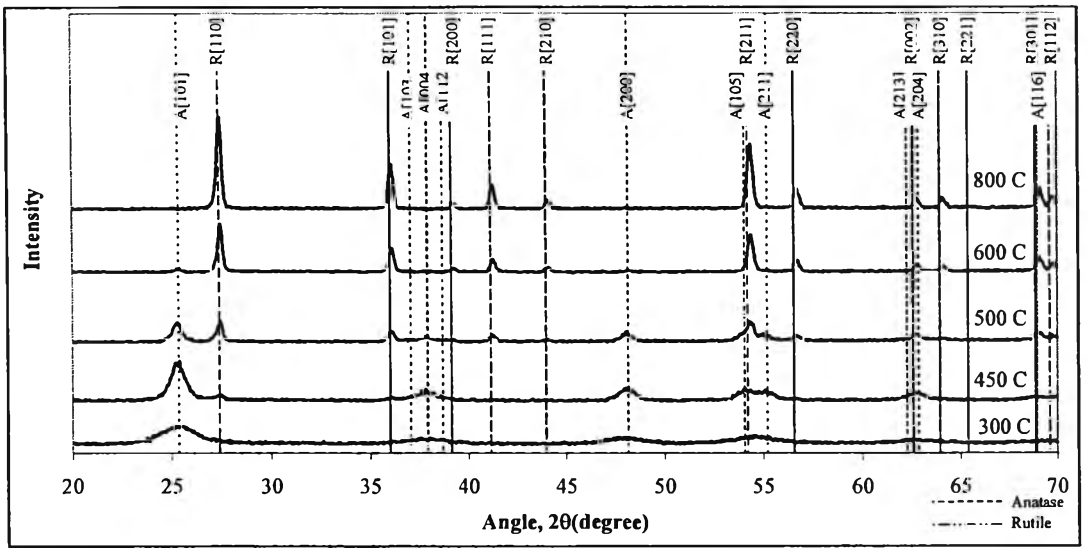

(a) TiO_2 without any stabilizing agents

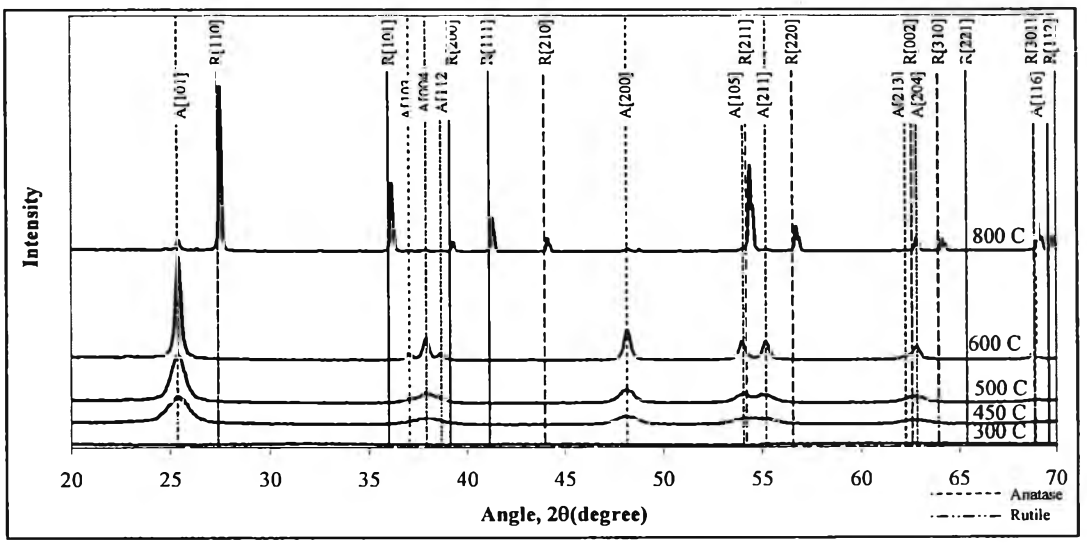

(b) TiO_2 with DEG

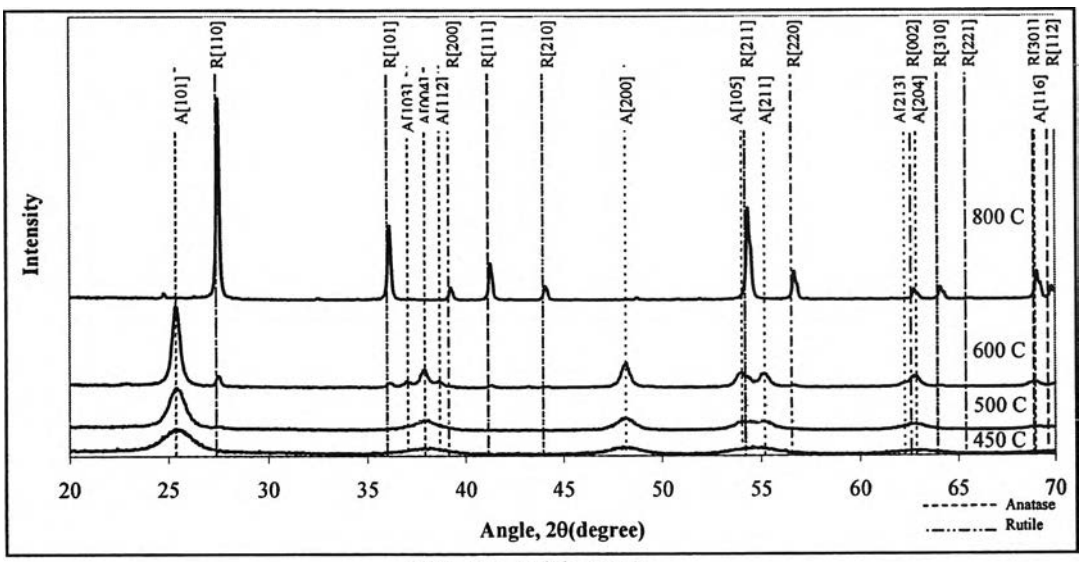

(c) TiO_2 with PEG

Figure 4.38 XRD patterns showing crystal structures of various nanocrystal TiO_2 after calcinated at temperature 300 - 800°C

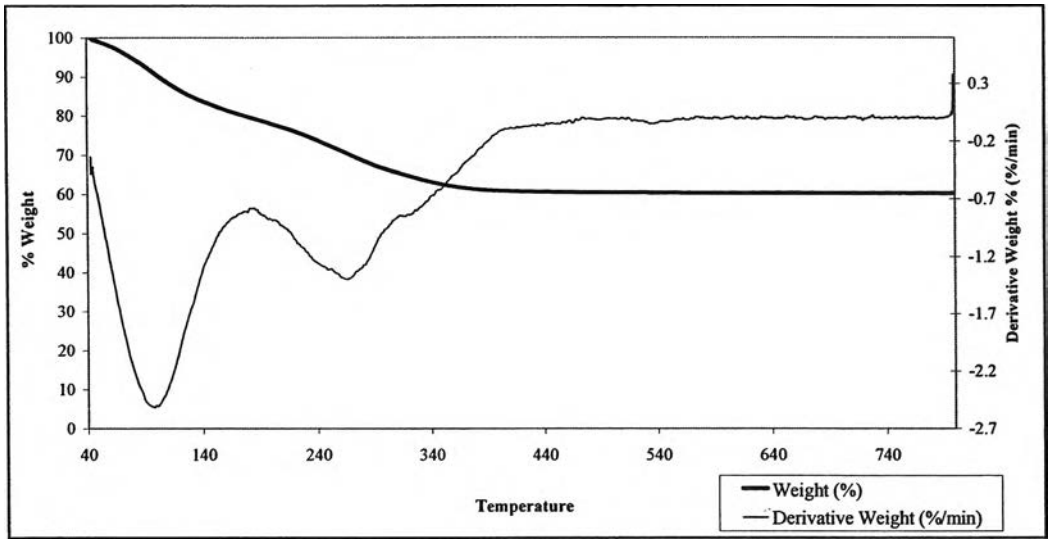

(a) TiO_2 without any stabilizing agents

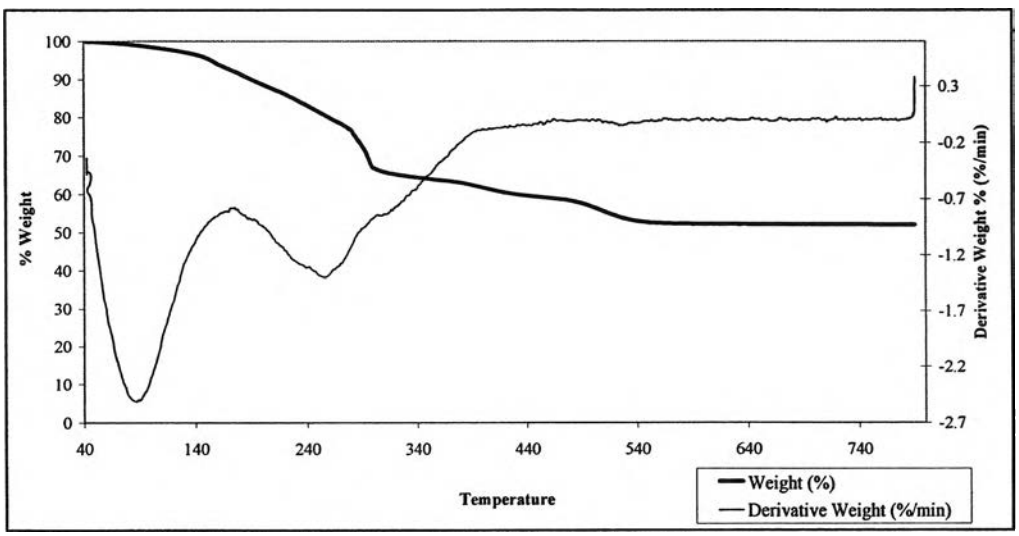

(b) TiO_2 with DEG

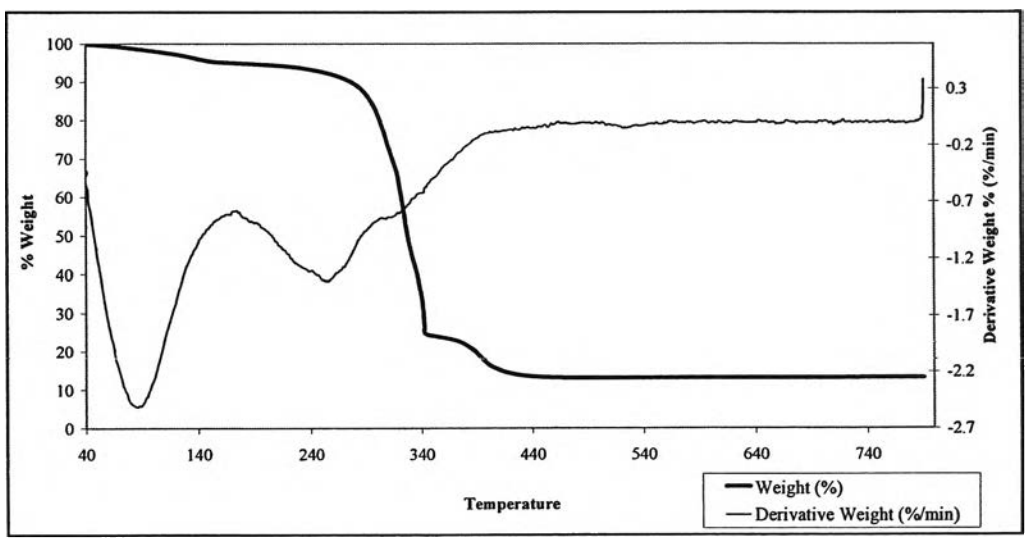

(c) TiO_2 with PEG 600

Figure 4.39 Thermo gravimetric analysis (TGA) of various types of TiO_2

It can be seen that, the weight loss proceeds in stages with increasing temperature. The most significant weight loss for these three preparation conditions, without any stabilizing agents, with DEG, and with PEG 600 occurred between 100-550°C. It is noted that there are two endothermic peaks in all three curves. The sharp and strong peak at approximately 100 °C and extended to 150 °C was attributed to the dehydration of absorbed water in the gel (Harizanov and Harizanova, 2000). The wide endothermic peak in the 150 – 340 °C temperature range may be caused by the decomposition of organic species such as alcohol in the gel. The wide exothermic peak in the range of 340-440 °C was due to the dehydration and combustion of organic substances contained in gel (Yu et al., 2000). Their positions and intensities were strongly dependent on the gel preparation process and its composition. This peak may correspond to the decomposition of organic additive (DEG or PEG 600) used in this work. In weight loss comparison, the percentages of weight loss of TiO_2 were 39, 48, and 87 % for TiO_2 without any stabilizing agents, with DEG and with PEG 600, respectively. It is obvious that the TiO_2 with PEG 600 had the highest percentage of weight loss. This may be due to the fact that PEG 600 has higher molecular weight compared to DEG. Moreover, PEG 600 was likely to be well decomposed below 440°C with the significant loss of PEG 600 itself. Thus, the TiO_2 after calcination temperature higher than 440 °C does not contain any residual organic substances in its crystal.

As DEG and PEG 600 exerted almost similar effects on TiO_2 nanocrystal, however, there are slight differences of TiO_2 properties obtained from DEG and PEG 600. Table 4.22 summarized the properties of TiO_2 prepared without any stabilizing agents, with DEG and with PEG 600.

When consider the effect of DEG and PEG 600 on the crystallite size of TiO_2, we chose to review 500 °C calcination temperature where nanocrystal TiO_2 were in anatase form. At this temperature, the crystallite size of TiO_2 with PEG600 is smaller than that of TiO_2 with DEG (18.40 nm and 20.82 nm, respectively). The surface area was also in an inversed proportion with crystallite size. As the size of TiO_2 was smaller the higher the surface area was obtained. The pore volume also tends to increase, whereas the pore diameter at this temperature also increased in case of TiO_2 with PEG 600.

Table 4.22 Properties of as-synthesized TiO_2 at various calcined temperature

Type of TiO_2	Calcined Temperature (°C)	Crystal Phase	Crystallite size (nm)	Surface area (cm^2/g)	Pore volume (cm^3/g)	Pore size (nm)
TiO_2 w/o stabilizing agents	300 °C	Anatase	9.31	174.5	0.0889	2.285
TiO_2 with DEG	300 °C	Amorphous	-	1.63	0.00421	9.391
TiO_2 with PEG 600	300 °C	Amorphous	-	1.58	0.005	1.501
TiO_2 w/o stabilizing agents	500 °C	Anatase (42.02 %) + Rutile (57.98 %)	31.03 (a) 56.18 (r)	22.2	0.03427	5.914
TiO_2 with DEG	500 °C	Anatase	20.82	82.25	0.09258	4.362
TiO_2 with PEG 600	**500 °C**	**Anatase**	**18.40**	**109.6**	**0.1393**	**4.969**
TiO_2 w/o stabilizing agents	600 °C	Anatase (11.59 %) + Rutile (88.41 %)	39.57 (a) 76.24 (r)	0.5187	0.002474	17.83
TiO_2 with DEG	**600 °C**	**Anatase**	**32.97**	**4.23**	**0.009124**	**8.055**
TiO_2 with PEG 600	600 °C	Anatase (86.52 %) + Rutile (13.48 %)	31.65 (a) 73.61 (r)	30.97	0.06122	9.797
TiO_2 w/o stabilizing agents	800 °C	Rutile	76.24	0.434	0.001501	12.67
TiO_2 with DEG	800 °C	Anatase (5.52 %) + Rutile (94.48 %)	83.30 (a) 164.21 (r)	3.11	0.025	15.25
TiO_2 with PEG 600	800 °C	Rutile	142.32	1.17	0.005	31.67

For TiO_2 with PEG 600, a single anatase phase was observed up to the 500 °C calcination temperature. However, rutile phase emerged for the powder calcined at 600 °C. At this calcination temperature, the anatase crystal phase of TiO_2 with DEG was relatively unchanged. The rutile phase in TiO_2 with PEG 600 contained crystals of a although the anatase phase of TiO_2 with PEG 600 was slightly smaller than that obtained from DEG. The surface area of nanocrystal TiO_2 with PEG 600 was 30.97cm^2/g while the surface area of anatase nanocrystal TiO_2 with DEG was 4.23 cm^2/g. The pore size of mixture phase in TiO_2 with PEG 600 at 600°C was also increased with the increasing of calcination temperature to 800°C.

At 800 °C calcination temperature, while TiO_2 without any stabilizing agents and TiO_2 with PEG 600 were fully rutile phase, the TiO_2 with DEG contained the mixture of a small portion of anatase and a bigger portion of rutile phase. Thus, TiO_2 with DEG provided the highest surface area of 3.11 cm^2/g and lowest pore size of 15.25 nm compared to TiO_2 from other preparation conditions.

The different effects of the DEG and PEG 600 in phase transformation at different temperatures might be explained by the short and long chains of polyethylene glycol in their molecules. The roles of PEG were described previously in the structure-directing process in PEG in the precursor sol by Zhang et al., 2003. In sol-gel system, water can exist as three forms: combined water, bonded water and free water. In the PEG chain, the water absorbed through hydrogen bond is called combined water, which makes the chain structure of PEG loose, thus providing enough room to hold bonded water. After the formation of combined water and bonded water, the leftover water is free water (Bailey and Koleske, 1990). At the beginning, titanium tetraisopropoxide (TTiP) might hydrolyze by free water and condensed to form sol particles. However, these particles cannot be fully covered by PEG chain. When further aged, TTiP will be hydrolyzed by the bonded water and combined water to form more particles. At the same time, the loose structure of PEG chains become tight after losing bonded water and combined water. Thus, the particles can be covered by PEG chains more tightly to form "particles–PEG" complexes. The resulting complexes then self-assemble through cross-linking and polymerization to form mesoscopically ordered inorganic/polymer composites (Sun et al., 2000). The whole process for a long chain PEG can be simply described as shown in Figure 4.40.

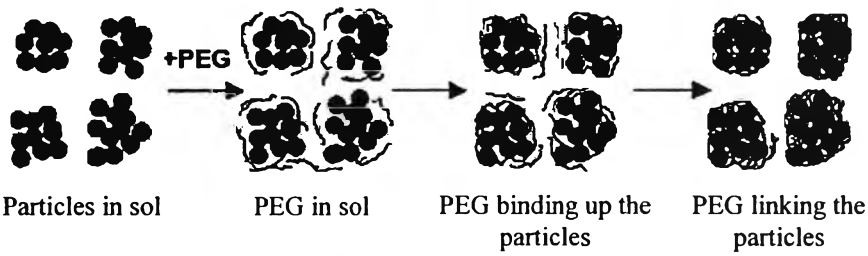

Figure 4.40 The structure-directing process of PEG in the precursor sol (Zhang et al., 2003)

As shown in Figure 4.39, the thermo gravimetric analysis (TGA) of TiO_2 with PEG, both DEG and PEG 600 were well decomposed at 440 °C calcination temperature. When organic decomposed, the residual holes of organic substances was left as porosity in the TiO_2 structure. Another comparison of DEG and PEG, the long chain of PEG 600 can agglomerate the nanocrystal TiO_2 more than the short chain of DEG. Thus, with the linkage particles, PEG 600 can accumulate the anatase and transform from the anatase to rutile phase at the lower temperature as compared to DEG, i.e. 600 °C for PEG 600 and 800 °C for DEG, as shown in Table 4.22.

4.3.2 Role of DEG and PEG 600 on photocatalytic activity

As DEG and PEG 600 affected the phase transformation from anatase to rutile, the photocatalytic activity of TiO_2 should be changed according to the existing phase of the nanocrystal. In previous work (Wang et al., 2003), it has been reported that the rutile phase of TiO_2 has a lesser photocatalytic activity than the anatase phase since the rutile phase possesses a slightly lower Fermi level and a lower degree of surface hydroxylation. In addition, excessive rutile phase is harmful to the photocatalytic activity of a powder, due to the large absorption coefficient and low photoactivity of the rutile phase (Wang et al., 2003).

To consider the role of DEG and PEG 600 on photocatalytic activity in chromium (VI) removal, the treatability of each type of TiO_2 prepared at difference calcination temperatures were compared. The efficiencies in chromium (VI) removal using different types of TiO_2 calcined at 300 °C are shown in Figure 4.41.

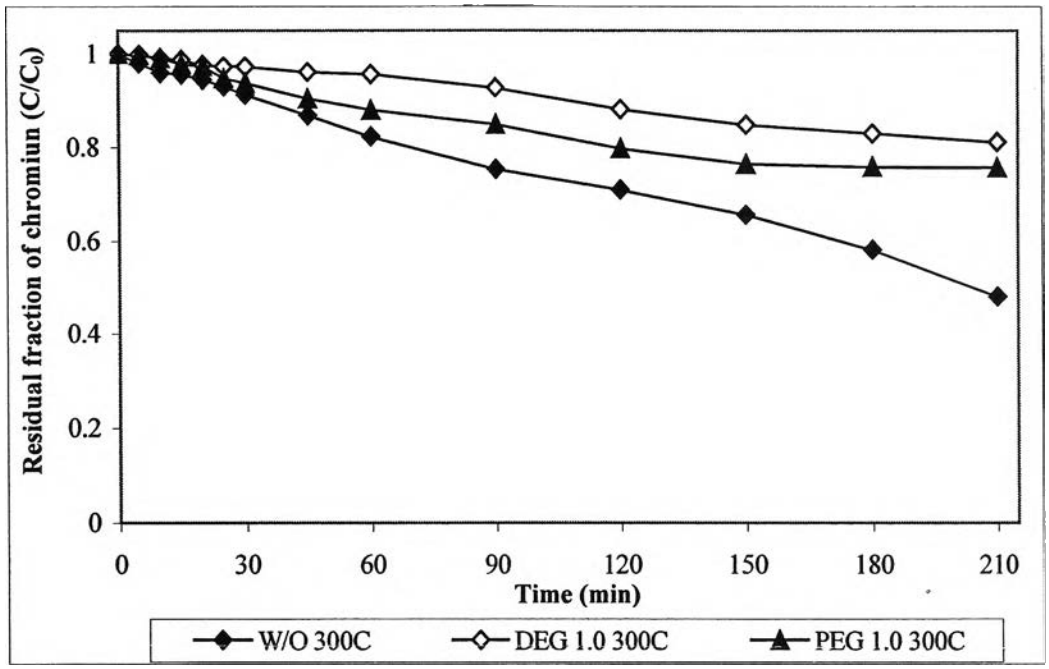

Figure 4.41 Efficiencies in chromium (VI) removal using different types of TiO_2 calcined at 300 °C

Figure 4.41 shows that TiO_2 without any stabilizing agents possesses the highest photocatalytic activity for the chromium (VI) removal among the three materials. This is due to the fact that the TiO_2 was anatase, while TiO_2 with DEG and with PEG 600 were in amorphous form. In addition, the TiO_2 without any stabilizing agents has the highest surface area compared to those two types of TiO_2 (see Table 4.22).

As the calcination temperature was up to 500 °C, the rutile was formed in the mixture phase of TiO_2 without any stabilizing agents, while both two types of TiO_2 with DEG and with PEG 600 were purely anatase. In addition, with higher molecular weight of PEG 600, the smaller in nanocrystal TiO_2 were formed when compared with DEG. This background information in TiO_2 properties were supported the reason that TiO_2 with PEG 600 performed the highest efficiency in chromium (VI) removal as presented in Figure 4.42.

At 600 °C calcination temperature, the long chain of PEG accelerated the agglomerate of anatase leading to the transformation from anatase to rutile phase as the rutile content in TiO_2 was 13.48 vol. %, while the short chain of DEG persisted with the anatase phase of TiO_2. The rutile content as of 88.41 vol. % was also existed in the mixture phase of TiO_2 without stabilizing agents. The comparison of chromium

(VI) removal efficiencies of different types of TiO_2 is shown in Figure 4.43. The TiO_2 with PEG provided the highest in chromium (VI) removal efficiency because of the pure anatase phase in TiO_2 crystals.

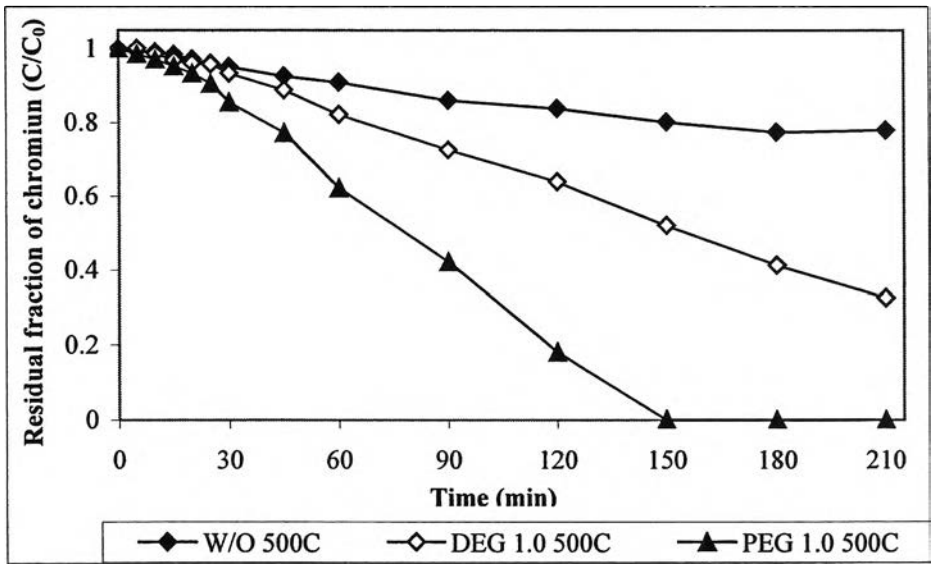

Figure 4.42 Efficiencies in chromium (VI) removal using different types of TiO_2 calcined at 500 °C

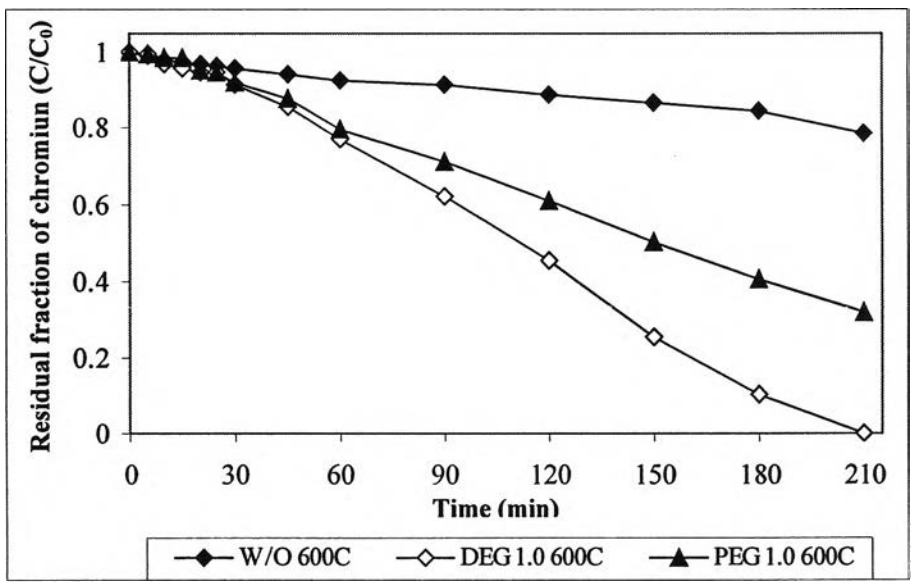

Figure 4.43 Efficiencies in chromium (VI) removal using different types of TiO_2 calcined at 600 °C

With the relatively high temperature of 800 °C, anatase phase in both TiO_2 without any stabilizing agents and TiO_2 with PEG 600 were fully changed to rutile phase while the mixed phase of anatase and rutile was seen in TiO_2 with DEG. The

rutile content in TiO_2 with DEG was 94.48 vol. % (Table 4.22). Thus, with rutile as the dominant crystal phase in all three types of TiO_2, the photocatalytic efficiency in all three cases are not considerably different (Figure 4.44).

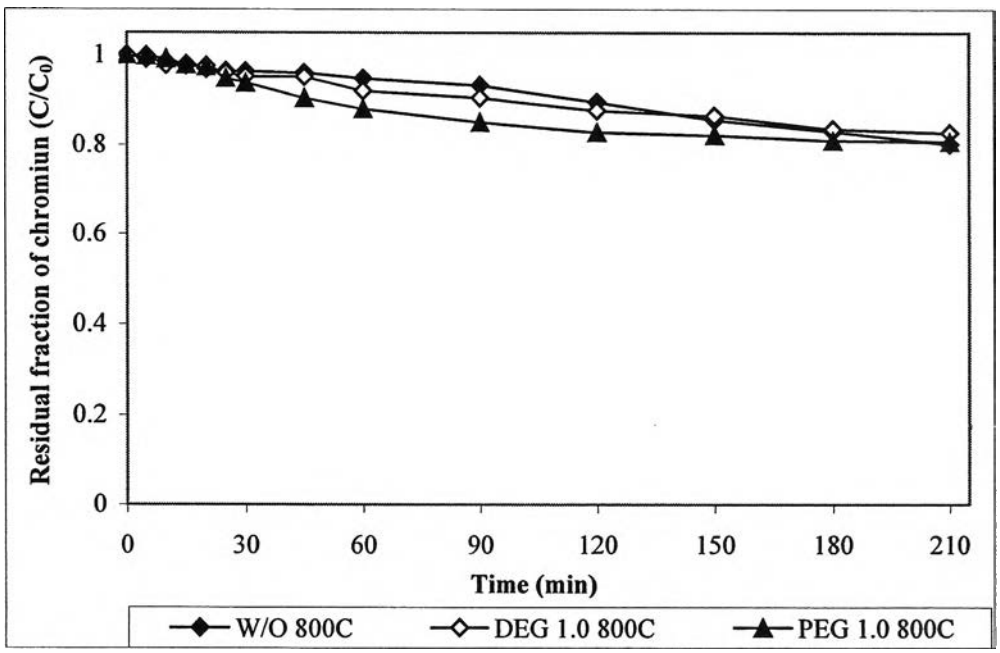

Figure 4.44 Efficiencies in chromium (VI) removal using different types of TiO_2 calcined at 800 °C

4.3.3 Role of DEG and PEG 600 on kinetic study of photocatalytic activity

As described in previous section (4.1 and 4.2) that the appropriate calcination temperature to synthesis TiO_2 with DEG and PEG 600 was found to be 600°C and 500°C, respectively The kinetic studies of photocatalytic activity in chromium (VI) removal for both conditions were calculated and compared in this section. The appropriate calcination temperature for TiO_2 without any additive was found at 300°C in which this condition provided the highest photocatalytic activity in chromium (VI) removal.

The photocatalytic activity of for TiO_2 in three conditions, without additive, with DEG and with PEG, are shown in Figure 4.45. It was found that the TiO_2 with PEG 600 has the lowest residual fraction chromium, therefore, provided the highest efficiency in chromium (VI) removal. It is worth to emphasize that in all three cases the crystal phase of TiO_2 were pure anatase phase. However, if comparing amount of

TiO_2 appear in each case, it was found that the content of anatase phase in TiO_2 crystal was in the order of PEG 600 > DEG > no additive. From above information, the highest amount of anatase presented in TiO_2 crystal and high surface area of TiO_2 obtained with PEG 600 addition might be the explanations that the TiO_2 with PEG 600 is the best photocatalyst.

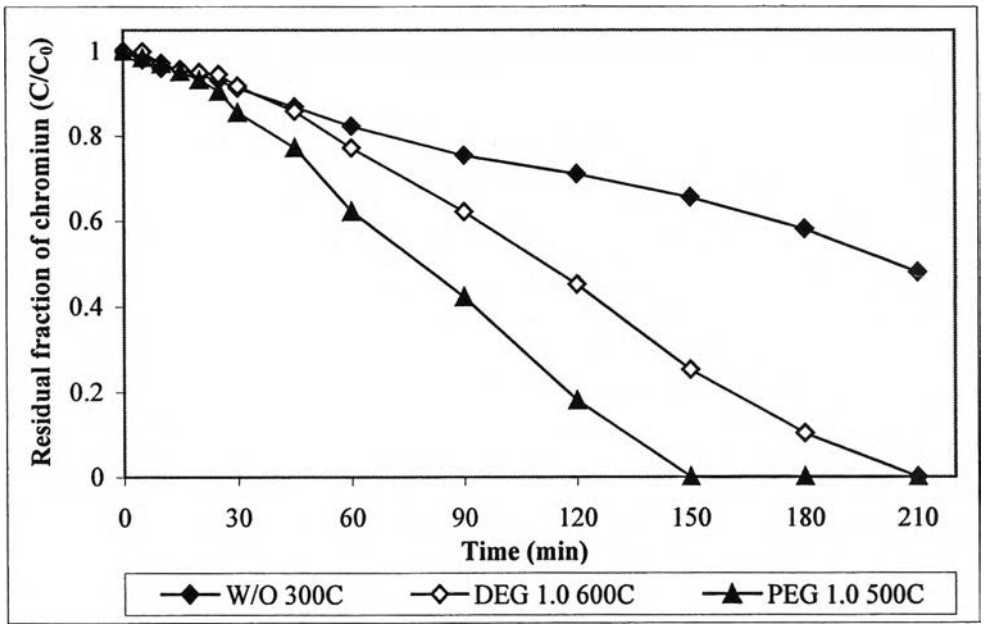

Figure 4.45 Efficiencies in chromium (VI) removal using different types of TiO_2 calcined at the best calcination temperature of each types of TiO_2

The values of k_c and K_{cr} of the three conditions, which were calculated following Langmuir-Hinshelwood model, were compared as shown in Table 4.23. Apparently, the TiO_2 with PEG 600 provided the highest value of K_{cr} representing the highest chromium (VI) adsorption on the surface of titania and the highest value of k_c illustrating the highest reaction rate in photocatalytic reduction of chromium (VI) upon irradiation process.

Table 4.23 Comparison of k_c and K_{cr} for three types of TiO_2

Types of TiO_2	k_c **mg/L-min**	K_{cr} **L/mg**
TiO_2 without additive	0.055	0.105
TiO_2 with DEG	0.168	0.287
TiO_2 with PEG 600	0.220	0.480